

2017

# Evaluation of aerogel as a material additive for the creation of synthetic defects in carbon fiber reinforced plastics

Zach Benedict  
*Iowa State University*

Follow this and additional works at: <https://lib.dr.iastate.edu/etd>

 Part of the [Aerospace Engineering Commons](#)

---

## Recommended Citation

Benedict, Zach, "Evaluation of aerogel as a material additive for the creation of synthetic defects in carbon fiber reinforced plastics" (2017). *Graduate Theses and Dissertations*. 16074.  
<https://lib.dr.iastate.edu/etd/16074>

This Thesis is brought to you for free and open access by the Iowa State University Capstones, Theses and Dissertations at Iowa State University Digital Repository. It has been accepted for inclusion in Graduate Theses and Dissertations by an authorized administrator of Iowa State University Digital Repository. For more information, please contact [digirep@iastate.edu](mailto:digirep@iastate.edu).

**Evaluation of aerogel as a material additive for the creation of synthetic defects  
in carbon fiber reinforced plastics**

by

**Zach Glenn Benedict**

A thesis submitted to the graduate faculty  
in partial fulfillment of the requirements for the degree of

MASTER OF SCIENCE

Major: Aerospace Engineering

Program of Study Committee:  
Vinay Dayal, Major Professor  
Ambar Mitra  
Stephen Holland

The student author, whose presentation of the scholarship herein was approved by the program of study committee, is solely responsible for the content of this thesis. The Graduate College will ensure this thesis is globally accessible and will not permit alterations after a degree is conferred.

Iowa State University

Ames, Iowa

2017

Copyright © Zach Glenn Benedict, 2017. All rights reserved.

## TABLE OF CONTENTS

	Page
LIST OF FIGURES .....	iv
LIST OF TABLES .....	vii
NOMENCLATURE .....	viii
ABSTRACT.....	ix
CHAPTER 1. INTRODUCTION.....	1
Common Types of CFRP Damage .....	1
Need for Synthetic Defect Samples .....	1
Current Methods for Fabrication of Synthetic Defects.....	2
Impacts.....	2
Foreign Body Inclusions (FBI).....	3
Delaminations .....	4
Aerogel Properties and Hypothesis.....	5
Objective of This Research.....	5
CHAPTER 2. EQUIPMENT.....	7
Ultrasonic Measurement .....	7
Thermography Measurement .....	10
Density Measurements.....	11
Aero-Epoxy Mixing Equipment .....	12
CHAPTER 3. MANUFACTURING PROCESSES.....	13
Film Inserts .....	14
Baking Soda Inclusions.....	14
Impact Damage .....	15
Teflon Insert for True Delamination.....	16
Aluminum Insert for True Delamination .....	17
Aerogel/Epoxy Simulated Delamination .....	18
CHAPTER 4. RESULTS.....	22
Initial Trials.....	22
Shape Control Trials .....	22
Signature Variability Test.....	27
Physical Characteristics .....	29
Similarity to Other Defect Types .....	33

CHAPTER 5. CONCLUSION .....	40
REFERENCES .....	42
APPENDIX: ADDITIONAL SAMPLE IMAGES.....	44
ACKNOWLEDGMENTS .....	50

## LIST OF FIGURES

	Page
Figure 1 (a) Signal With and Without Damage, (b) Back Wall and Damage Signal Reflections, (c) Contact Measurement Setup, (d) Water Immersion Setup.....	7
Figure 2: Transducer Frequency and Size Comparison.....	8
Figure 3: Through-Transmission Ultrasound Setup Scheme.....	9
Figure 4: Beginning of Signal from TTU .....	10
Figure 5: Basic Thermography Setup .....	10
Figure 6: Density Measurement Setup.....	11
Figure 7: Composite Vacuum Bag Assembly Diagram.....	13
Figure 8: Film Insert Layout Diagram .....	14
Figure 9: Baking Soda Layout Diagram .....	14
Figure 10: Impact Sample Diagram.....	15
Figure 11: Teflon Insert Delamination Diagram .....	16
Figure 12: Aluminum Insert Delamination Diagram.....	17
Figure 13: Aero-Epoxy Manufacturing Flow Chart .....	19
Figure 14: Immersion Scan Results of First Aerogel Trial (5 MHz Left, 10 MHz Right) .....	22
Figure 15: a.) Aero-Epoxy Sample Prior to Assembly b.) Immersion Scan Results Aero-Epoxy Panel.....	23
Figure 16: a.) Partially Cured Mixture and Epoxy Prior to Assembly b.) Immersion Scan of Panel c.) Thermographic Scan of Panel.....	24

Figure 17: a.) Solid Aero-Epoxy and Pure Epoxy Sheets On Midplane Prior to Assembly b.) Immersion Scan of Solid Epoxy Sample c.) Thermographic Scan of Solid Epoxy Sample.....	25
Figure 18: Progression of Aero-Epoxy Viscosity a.) Less Than 1:1 b.) Between 1:1 and 1:2 c.) 1:2 and Greater.....	26
Figure 19: A-Scan Comparison of Aero-Epoxy Ratios .....	27
Figure 20: Graph of Amplitudes of Damage Signals and Backwall Signals for Aero-Epoxy Ratios.....	27
Figure 21: Example of Uniform Signature in Aero-Epoxy Samples a.) 1:1 b.) 1:1.5 c.) 1:2 .....	28
Figure 22: Immersion Scan Showing Variability of Signal Using Multiple Aero-Epoxy Ratios.....	28
Figure 23: Diagram of Acoustic Reflection at Material Interfaces.....	30
Figure 24: Wave Speed of Aero-Epoxy as Aerogel Ratio Increases .....	31
Figure 25: Microscopy of Aerogel Particles and Aero-Epoxy Samples.....	32
Figure 26: Visual Comparison of Film Insert Defect and Solid Sheet Aero-Epoxy Sample.....	33
Figure 27: Difference in Apparent Amplitude Based on Color Grading.....	34
Figure 28: Signature Comparison of Film Insert, 1:0.8 Aero-Epoxy, and 1:1 Aero-Epoxy Samples.....	34
Figure 29: Visual Comparison of Baking Soda and Partially Cured Aero-Epoxy Samples.....	35

Figure 30: Signature Comparison of Baking Soda, 1:0.8 Aero-Epoxy, and 1:1 Aero-Epoxy Samples.....	36
Figure 31: UT Inspection Results of a Blunt Impact on CFRP (B-Scan, C-Scan, A-Scan Left to Right).....	36
Figure 32: Visual Comparison of Teflon Delamination, Aluminum Delamination, and .....	37
Figure 33: Micrograph of Delamination .....	38
Figure 34: Signature Comparison of True Delamination and Aero-Epoxy Simulated Delamination.....	39
Figure 35: Signature Comparison of True Delamination and 1:1 Aero-Epoxy.....	39
Figure 36: Pulse/Echo UT C-Scans of Additional Film Insert Samples.....	44
Figure 37: Pulse/Echo UT C-Scans of Additional Baking Soda Samples.....	45
Figure 38: Pulse/Echo UT C-Scans of Additional Aluminum Delamination Samples .....	45
Figure 39: Pulse/Echo UT C-Scan of Additional 3J Impact Sample.....	46
Figure 40: Pulse/Echo UT C-Scans of Various Ratios of Aero-Epoxy Samples .....	46
Figure 41: Various Thermography Scans of Samples .....	48

LIST OF TABLES

	Page
Table 1: Properties of Aero-Epoxy .....	31



## NOMENCLATURE

Pre-Preg: Composite sheets that are pre-impregnated with epoxy resin for composite manufacturing.

Ply: A single layer of a composite.

Laminate: A sum of plies that forms a composite panel.

NDE: Non-Destructive-Evaluation

Tup: Metal impactor

FBI: Foreign-Body-Inclusion

CFRP: Carbon Fiber Reinforced Plastic

MTS: Tensile testing machine.

TTU: Trough-Transmission-Ultrasound

ToF: Time-of-Flight

PPE: Personal-Protective-Equipment

Aero-Epoxy: The mixture of Aerogel and Epoxy Resin

UT: Ultrasonic Testing

## ABSTRACT

Damage within CFRP composites (commonly used in the aerospace industry) is often difficult to locate and identify, often occurring beneath the surface of the material. Many methods are used in an attempt to isolate these unseen defects, from thermography to a wide array of ultrasonic techniques. Real damage can be used to train personnel and calibrate inspection equipment, however synthetic damage is favorable for the same uses as it can be manufactured at will to any specification desired. Current methods are capable of creating foreign body defects, impact damage, and delaminations, however these methods can require expensive equipment and/or a great amount of time to manufacture. Aerogel was investigated to determine if the material could be used to simulate several types of damage common to CFRP. Samples were created by mixing Aerogel and Epoxy Resin and placing it within composite laminate layups. These samples were used to determine the material characteristics of Aerogel in relation to NDI and the response of the material under UT and Thermographic inspection. The Aerogel/epoxy mixture was optimized to achieve best ultrasonic response which could be a replacement of delamination. It was found that Aerogel was not only ultrasonically visible within the composite panel samples but had a pronounced signature compared to pure epoxy. By altering the amount of Aerogel used, the shape and size of the artificial defects could be controlled. Comprehensive scans of the samples revealed that Foreign Body Inserts (FBI) and delaminations could be matched almost exactly in UT signature and physical appearance, therefore the Aerogel method could be used in place of the current methods. Though in terms of time and cost the original method was better for creating FBIs, substantial savings could be attained with the Aerogel methods when creating synthetic delaminations.

## CHAPTER 1. INTRODUCTION

### Common Types of CFRP Damage

Carbon fiber composites, like any other material, can accumulate damage while in service. In-service damages typically come in the form of delaminations (Agarwal) and/or matrix cracking caused by excessive loading or impacts, such as excessive bending of a wing of an aircraft during a High-G maneuver or the accidental drop of tooling onto a composite surface during routine maintenance. However, defects can also occur during the manufacturing process (Garrett). While assembling the laminate, it is possible to leave behind portions of the backing paper found on pre-preg sheets in between the plies or contaminate the ply surface with dust or oils if the assembly environment is not properly maintained or the fabricator is not careful. These internal defects can occasionally go unnoticed, as they are not externally visible, yet still having a dramatic detrimental impact on the stiffness and strength of the laminate (Garrett) that can lead to catastrophic in-service failure.

### Need for Synthetic Defect Samples

In order to detect internal defects or existing damage, a suite of NDE techniques are widely used. Mechanics of composites (Tsai) shows that unlike isotropic materials, stresses inside a composite can be larger than the surface stresses and as a result the damage can occur inside the laminate while the outside surface remains pristine. This is especially true for low velocity impact on composites and these flaws cannot be detected by visual inspection. Hence advanced NDE methods such as ultrasound and thermography are needed to evaluate such damage. Thermographic inspection is commonly used to scan large areas to locate and define defects with relative ease and expediency. When the damage has been

found, or if the part is relatively small, Ultrasonic inspection is employed to generate a highly accurate profile of the defects and their location, which can then be isolated, defined, and repaired (International, E2533-17 Standard Guide for Nondestructive Testing of Polymer Matrix Composites Used in Aerospace Applications). However, before any NDE inspection it is necessary to possess the knowledge of what signal constitutes “damage” in regard to the data collected from the NDE tools. By scanning laminates where the location, size, and type of defect is known one can quickly designate what is damage and what is not. Therefore, proper methods of creating synthetic damage that is representative of real world damage is vital to the training and detection process. Impact damage, delaminations, foreign bodies, etc. all have their own individual signatures and possessing reference standards containing synthetic versions of these allows for an NDE investigator to decipher what is the problem with any given laminate they are inspecting and how to best address the problem. Standard samples are also helpful in the calibration of inspection equipment used in the field. A standard calibration sample is also very useful in the training of the inspector who can learn to differentiate between different defects and then use this knowledge on actual structures. Inspection is a time-consuming process and any training in a controlled environment with controlled samples is typically cost effective.

#### Current Methods for Fabrication of Synthetic Defects

This work is restricted to three types of synthetic defects: Barely-visible impact, foreign-body inclusion and delamination. Each one is defined as follows.

##### Impacts

In composite materials, if the impact energy is high then the impactor will cut into the fibers or crush the matrix. This type is visually detectable and further investigation is

straightforward. On the other hand, if the impactor is blunt and impact energy is low, the damage may be barely visible or unable to be seen at all. This damage would generally be in the form of matrix crushing, and some delamination can occur. Impact due to blunt tool drop or bumping of service carts on the fuselage are typical in day to day service and operation of aircrafts. The extent of such damage is important to know because even though this defect is not catastrophic, it can become the nucleation site for damage growth. Also, such damage will change the local stiffness which can alter the response of the structure (Garrett). In damage of this type, the extent of damage is measured and then repairs are performed. Impact damage is typically created by simply impacting a CFRP sample with a metal Tup designed to replicate specific types of impactors, such as hemispherical blunt impacts or chisel type sharp impacts. The amount of energy with which the Tup impacts the laminate can be easily altered by simply raising the drop height of the impactor. This system allows a wide variety of impacts to be recreated from barely-visible-damage to obvious matrix cracking at the impact site.

#### Foreign Body Inclusions (FBI)

If using pre-preg sheets of carbon fiber, the sheets typically come with a backing paper layer designed to keep the layers of carbon from adhering to each other. This layer must be removed prior to assembly of the laminate. Sometimes, however, the backing paper can tear while peeling it off, and a small piece can be left behind that will then remain imbedded inside of the layup if the manufacturer is not paying close attention. If the environment in which the composites are being fabricated is not maintained well, it is also possible for contaminants of all kinds to find their way into the laminates. Depending upon what type of body, the manufacturing process can change slightly for the manufacturing of

synthetic FBIs, but in general it comes down to simply placing the inclusion as desired within the laminate during layup and curing the panel with the defect inside of it. Film, paper, or bagging fabric inserts are used to simulate manufacturing material mishaps while powders such as baking soda are used to simulate more amorphous inclusions. The effect of FBI is separation of the plies which results in reduced stiffness and nucleation of further defect growth.

### Delaminations

Generally, delamination is not the initial damage in composites. The damage initiates in the form of micro-cracks in the matrix (K.L. Reifsnider). Micro-cracks develop in a ply due to other damage mechanisms, but then due to fiber orientation are unable to extend into next ply. Further input of energy turns these micro-cracks at a perpendicular angle and results in delamination occurring between laminas. These delaminations can grow undetected and can result in catastrophic failure of the entire composite laminate. Hence it is very important to detect and quantify the location and size of delaminations as early as possible. Keeping in theme with the simplicity of how damages can be created within reference standards, delaminations are usually created by quite directly peeling apart a cured CFRP panel. During the layup process a material is placed at the desired delamination plane to stop adhesion and serve as a starting point for the delamination. Once cured, hinges are attached on the end containing the insert and the panel is pulled apart using an MTS machine or other tensile testing machine. Once the delamination has progressed past the insert the sample is ready for use (International, D6115-97 Standard Test Method for Mode I Fatigue Delamination Growth Onset of Unidirectional Fiber-Reinforced Polymer Matrix Composites). The only restriction of this method is that the delamination can be formed on an edge of the sample. To

produce more realistic delaminations we have experimented with the use of Aerogel within the lamina for reasons to be discussed shortly.

### Aerogel Properties and Hypothesis

Originally created in the 1930's, Aerogel has been used in a suite of applications due to its peculiar properties. For one, it possesses an extremely low density as it is 98.2% air by volume. It also possesses a low thermal conductivity, which has led to it being utilized as a thermal insulator (Hrubesh). It has a Hydrophobic coating, since it degrades quickly in water, and is quite brittle. Of particular interest to NDE, it has a low acoustic impedance (A. Soleimani Dorcheh) with some silica Aerogels reaching as low as  $7000 \frac{kg}{m^2s}$  (the acoustic impedance of air is  $429 \frac{kg}{m^2s}$ ). Due to these properties, it was hypothesized that when placed in a laminate it would be possible for it to possess a similar damage signature as a delamination.

### Objective of This Research

The goal of this research was to determine if Aerogel could indeed be used as a material additive to create synthetic delamination damage and possibly even other types of synthetic damage as well. There were a few initial issues with the material itself that had to be overcome, however. Aerogel is a very low-density material and as such the powdered form of the material easily floats in air if disturbed in the slightest. Inhalation of aerogel can be detrimental to the health of the fabricator, so protective equipment designed to prevent the Aerogel from being loosed into the environment and prevent its inhalation by personnel was needed. Also, when the aerogel powder was placed in between the laminas it was observed that the amount of aerogel and the shape of intended delamination was difficult of control. Aerogel would just float away as soon as pressure was applied to the ply and only a very thin

layer would stay adhered to the surfaces. To attempt to contain the particles, it was decided to mix aerogel with epoxy to make a low density paste which could be easily controlled and simultaneously reduce the health hazard it presented previously. The proper ratio of aerogel to epoxy, the extent of pre-curing of the epoxy before it could be placed between laminas, and the signature of the ultrasonic and thermographic interrogation are the subject of this work and are described next.



## CHAPTER 2. EQUIPMENT

## Ultrasonic Measurement

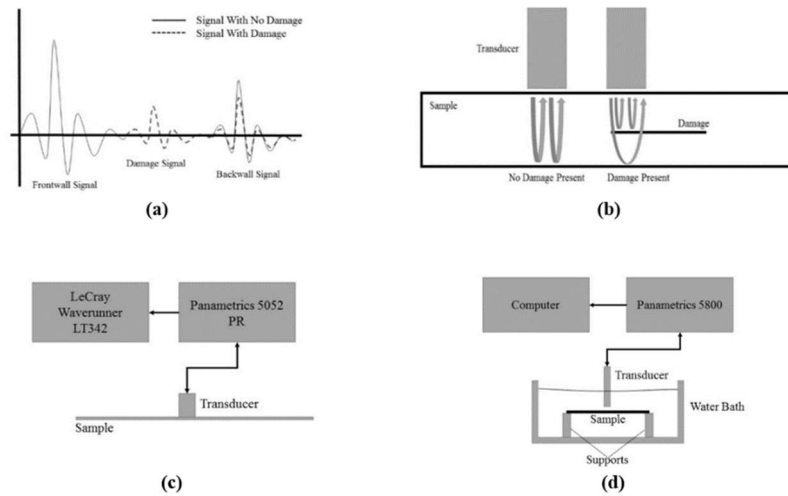


Figure 1 (a) Signal With and Without Damage, (b) Back Wall and Damage Signal Reflections, (c) Contact Measurement Setup, (d) Water Immersion Setup

The majority of the data was collected using ultrasonic NDE techniques including Water-Based Immersion Scanning, Point by Point Contact Scanning, and Through Transmission Scanning. When performing immersion scans, the sample was placed in a basin filled with distilled water upon a pair of aluminum blocks to separate it from the bottom of the basin for purposes of isolating the sample signal from the signal coming from the surface of the basin floor. The transducer was mounted on an automated mechanical traverse, and was connected to a Panametrics 5800 Signal Generator, which was in turn connected to a computer from which entire operation was controlled. The step size of the scan in both the horizontal and vertical directions was 0.04 inches. This method was used to obtain representative images of entire samples and for point by point A-Scan capturing for comparing damage signals and backwall attenuation between the various samples. For all

water immersion scanning, a 0.25" diameter 5 MHz probe in Pulse/Echo mode was used. This probe was selected after exploring the effects that the size (diameter) and frequency of probe had on the clarity and accuracy of the defect images.

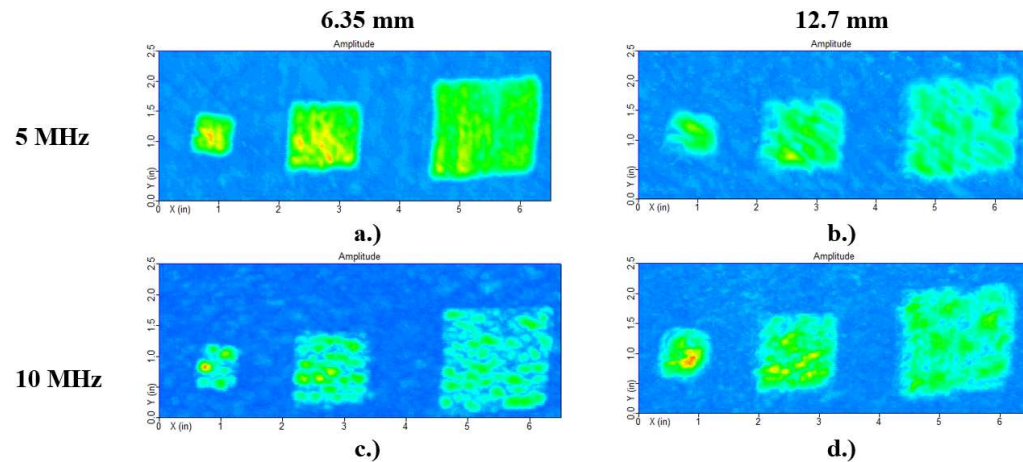


Figure 2: Transducer Frequency and Size Comparison.

At higher frequencies scattering becomes more prominent due to the short wavelength and larger diameter probes average data over a larger area and are therefore more prone to “blur” pixels near the edges of defects leading to a larger apparent size of inclusions and other damages. For this reason, the 0.25 in diameter 5 MHz probe was used for UT Immersion investigation.

For contact scans, a Panametrics 5052 Pulser-Receiver was used with a LeCroy Waverunner LT342 Oscilloscope and a 0.25" 5MHz contact probe to gather point by point data. This was initially the main source of Time of Flight data using Pulse/Echo mode, but as the scattering and attenuation of signals increased the ability to accurately determine the time of the first signal reception. Through-Transmission-Ultrasound (TTU) was employed in order to attain usable, clear measurements of the samples.

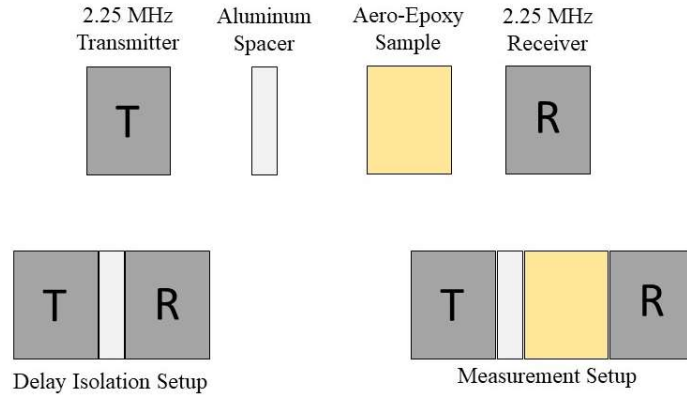


Figure 3: Through-Transmission Ultrasound Setup Scheme.

The TTU system used in this research consisted of a 2.25 MHz Transmitter Probe and a 2.25 MHz Receiver Probe connected to the Panametrics 5800 signal generator and the computer used for immersion scanning. TTU was primarily used for determining wave speeds, by measuring the ToF through sample blocks made from the materials used to create synthetic defects. To account for the inherent delay in the system and the time required to pass through the aluminum delay block, the following subtraction was made.

$$\text{Recorded } ToF_{\text{Aluminum}} = ToF_{\text{Aluminum}} + \text{Delay}$$

$$\text{Recorded } ToF_{\text{Sample}} = ToF_{\text{Block}} + ToF_{\text{Aluminum}} + \text{Delay} = ToF_{\text{Block}} + \text{Recorded } ToF_{\text{Aluminum}}$$

$$ToF_{\text{Block}} = \text{Recorded } ToF_{\text{Sample}} - \text{Recorded } ToF_{\text{Aluminum}}$$

The first deviation from the background or “base” signal was considered the time at which the signal was received (see Figure 4).

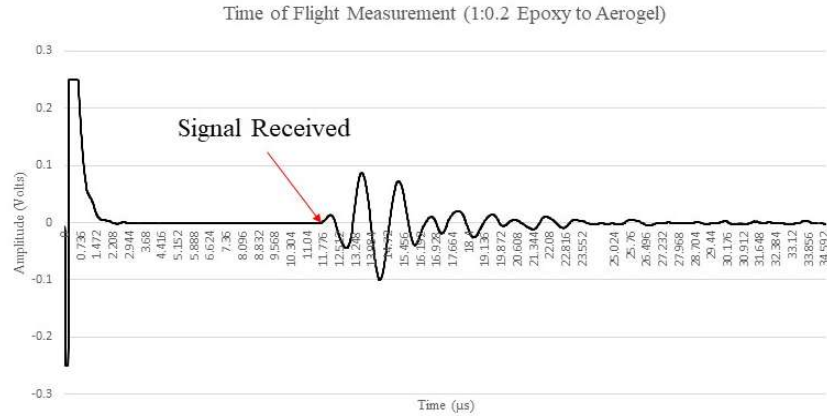


Figure 4: Beginning of Signal from TTU

### Thermography Measurement

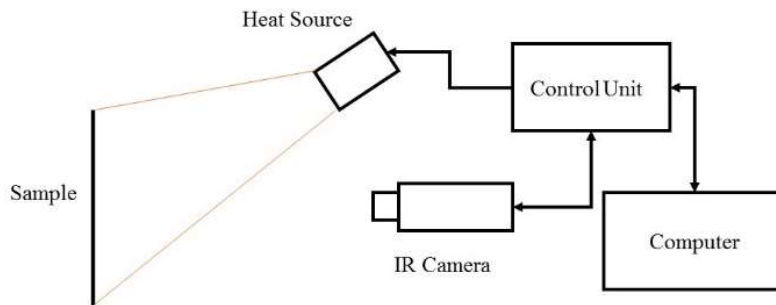


Figure 5: Basic Thermography Setup

All composite panel samples, in addition to being subjected to Ultrasonic scanning, underwent Thermographic scans. The objective was to capture whole field images of the samples, examine and compare defect signatures under thermography inspection, and to achieve coverage of further inspection methods used in industry. The simplified setup includes a computer that controls the timing/control unit connected to the infrared imaging camera and the heat source (in this case a high-intensity flash bulb at  $10\text{-}20 \frac{\text{kJ}}{\text{m}^2}$ ).

## Density Measurements

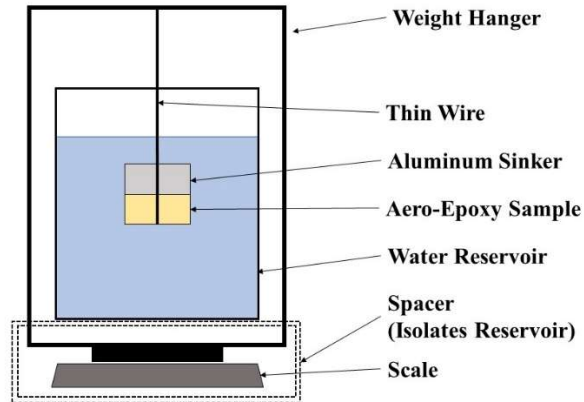


Figure 6: Density Measurement Setup

As part of the impedance measurement process it was necessary to determine the density of each of the Aero-Epoxy sample blocks as well as a pure epoxy control block. From Archimedes principle, the volume of the samples could be determined by finding the difference between the mass of the sample dry in air and its apparent mass when submerged in water. However, since most of the samples were less dense than water, they would float. So a sinker was added to weigh down the samples so they would stay submerged during measurement. With the sinker factored in, the equation used to determine the volume of each sample is included below:

$$Vol_{Block} = \frac{(Mass_{Block} + Mass_{Sinker})_{Air} - (Mass_{Block} + Mass_{Sinker})_{Water}}{\rho_{Water}} - Vol_{Sinker}$$

A Sartorius Analytic scale (accuracy up to 0.0001 grams) was used to measure the mass, however it had a mass limit of 200 grams meaning the water basin had to be isolated from the scale. Figure 6 shows the setup of the mass measuring process. The water itself was

distilled and subjected to a vacuum to eliminate the likelihood of air bubbles forming on the samples, as they could affect the accuracy of the measurement. All measurements reported are the average of three measurements.

#### Aero-Epoxy Mixing Equipment

An SOS20-S stand mixer was used to mix together the aerogel (Enova IC3100) and epoxy (US Composites 3:1 Epoxy Hardener and 635 Thin Epoxy Resin or INF-211 and INF-114 Thin Resin) so it could be easily applied to the composite panels for defect manufacturing. Standard 12-ounce plastic cups with lids containing straw holes were used to hold the materials during the mixing process. The hole in the lid was convenient for passing the stirring rod shaft through while still sealing the cup and preventing aerogel egress during the mixing process. All equipment involved in mixing were held within a negative pressure fume hood for the safety of the operators due to the health hazards particulate aerogel poses. The instruments were cleaned with acetone to keep epoxy buildup from occurring on the stirring surfaces. The PPE worn included nitrile gloves, safety glasses, and a half (or full) mask respirator with cartridges capable of handling small particulates and organic solvents.

## CHAPTER 3. MANUFACTURING PROCESSES

Most samples manufactured for this research were of the same 32 ply bi-axial layup sequence  $[(0_2/90_2)_4]_s$  and were made using the same composite pre-preg, TORAY T800SC-24000. The typical sample size was 6" by 6" (prior to pressing). There were a few deviations from this on occasion as the need arose. A few samples were made with reduced thickness of 16 plies at  $[(0_2/90_2)_2]_s$  to achieve clearer scans with thermography as the thickness of the 32 ply samples and the depth of the defects would sometimes prevent a clear image of the damage. Some samples were produce as 4" by 4" instead of the 6" by 6" variety to conserve space on the press and allow for a few samples to be made at once instead of just one per curing cycle. Due to the geometry constraints of the impact testing machine, the impact samples were 8 plies and 6" by 4" rectangles. Figure 7 shows the standard bagging system used when curing the composites.

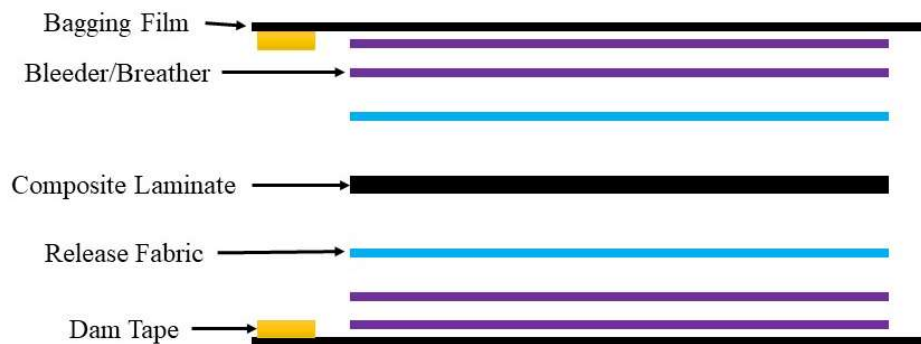


Figure 7: Composite Vacuum Bag Assembly Diagram

### Film Inserts

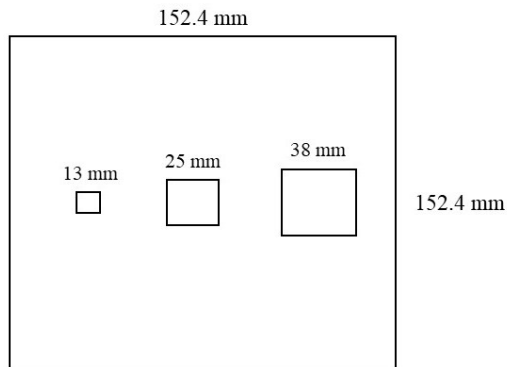


Figure 8: Film Insert Layout Diagram

The laminate was completed up to the midplane, at which point three pieces of vacuum bagging film were cut and placed on the laminate in the order and arrangement as shown above in Figure 8. Each film piece was cut in a rectangular shape and folded over on itself to form a square double the thickness. The open side of the fold was placed facing the same direction for all inserts, then the first ply of the top half of the layup was carefully pressed down from the closed side to the open side of the fold to make sure the film laid down closed in the square shape. The three sizes were 0.5 in, 1 in, 1.5 in squares.

### Baking Soda Inclusions

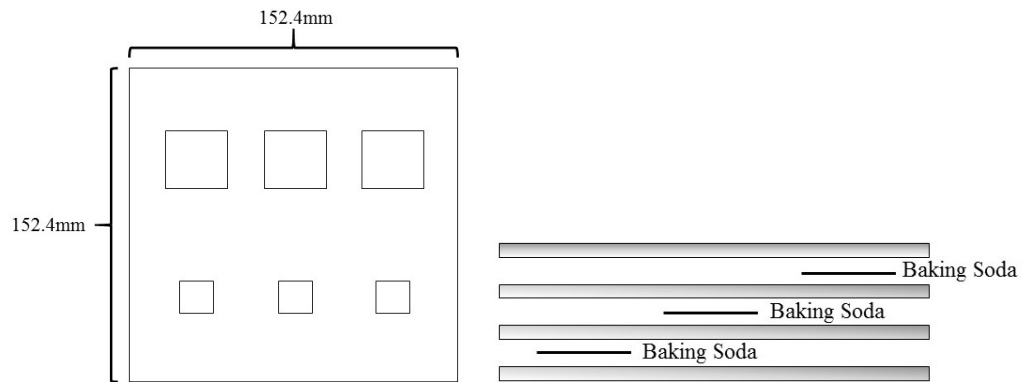


Figure 9: Baking Soda Layout Diagram



To recreate excessive dust or contaminant inclusion, baking soda (due to it being non-reactive with CFRP) was applied to the midplane of the laminate during fabrication. Small amounts of baking soda were gently lowered on to the pre-preg so as to avoid it scattering on impact. If desired it could then be spread around or shaped by applying a paper template before spreading the baking soda, then gently lifting the paper when coverage has been achieved. Once in place, the next ply was carefully lowered onto the panel and lightly pressed into place around the edges of the laminate before applying firmer pressure with the roller and continuing with fabrication of the rest of the layup.

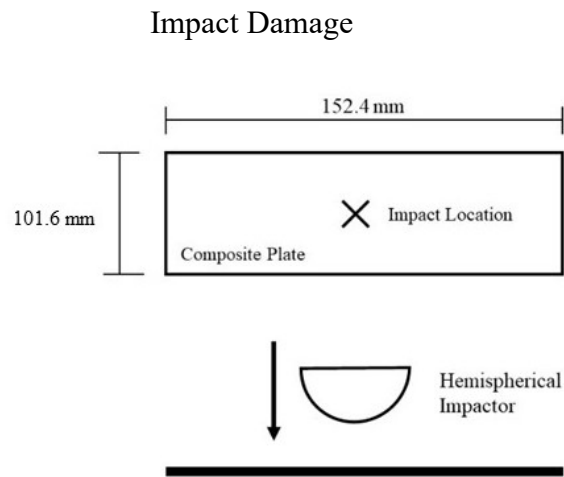


Figure 10: Impact Sample Diagram

An Instron Dynatup 8200 Drop Tower was used with Hemispherical 15.9mm Diameter Steep Impactors to create the barely visible impact damage in each of the CFRP samples. The input energy was three joules for most tests, unless otherwise stated. The tups were dropped onto the face of the laminate from a sufficient height for a 3J impact energy then caught to prevent secondary impacts from occurring. Samples were scanned with the immersion scanner, before and after the impact loading.

## Teflon Insert for True Delamination

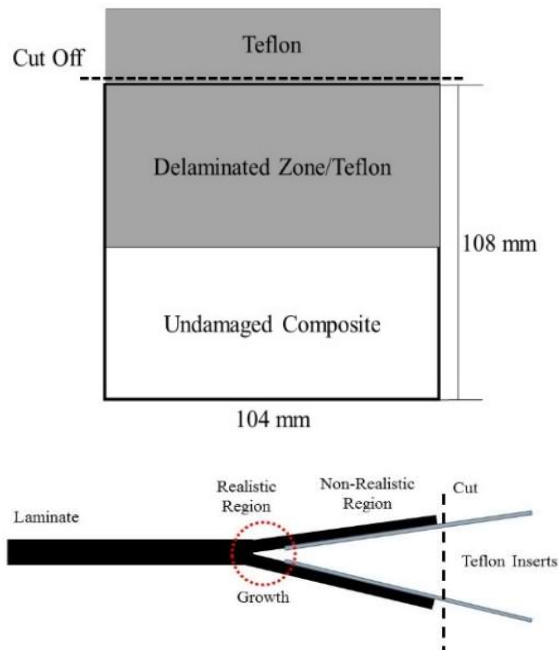


Figure 11: Teflon Insert Delamination Diagram

To begin the process of creating a true delamination, a Teflon insert was placed on the edge of the midplane of the pre-preg panel (4" by 4"). The Teflon serves as a starting point for a delamination when the panel is later subjected to tensile loading perpendicular to the Teflon plane. The rest of the laminate was then assembled, bagged, and pressed as per normal procedure. Once curing was complete, metal door hinges were glued onto the edge of the sample containing the Teflon insert using a structural adhesive. When set, the panel was taken to an tensile testing machine and affixed via the hinges and pulled until the panel peeled apart about an inch or so past the edge of the Teflon. To finish the process, the excess Teflon was then removed. This leaves the panel with an "insert" region filled with the Teflon, and a "realistic" region where the panel has separated as in a true delamination. The biggest detriment to this method is the amount of time required to manufacture a single panel. 4-6 hours to manufacture and press a panel, 8-16 hours for assembly and setting of the

adhesive for the hinges, and about an hour for separation of the plies. A much quicker method for fabrication was quickly sought out.

### Aluminum Insert for True Delamination

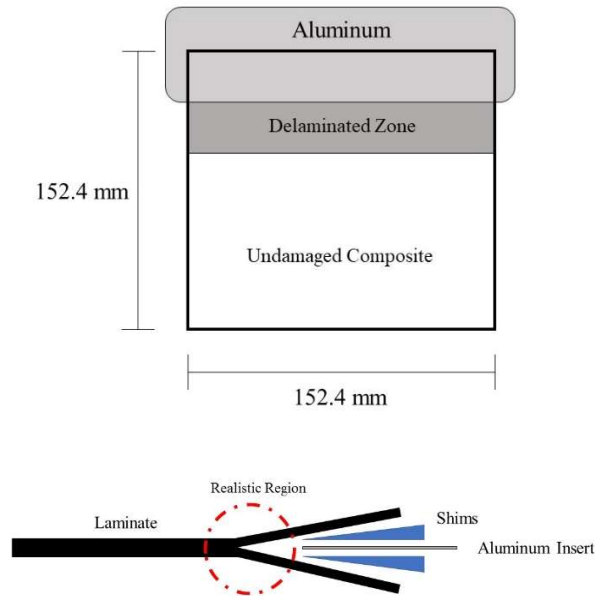


Figure 12: Aluminum Insert Delamination Diagram

In an effort to reduce the amount of time and machinery required to manufacture delamination samples, a new approach was considered. In place of the Teflon insert an aluminum sheet (about 0.01" in thickness) was used. However, before placing it at midplane, the sheet was coated with Fiberglass and FreKote to inhibit the adhesion of the pre-preg matrix to the sheet itself while the panel cures. When cured a noticeable separation could be seen at the interface between the aluminum and the panel. It is at this location that metal shims are placed and the panel is manually split apart past the edge of where the aluminum was originally placed (in the same way as with the Teflon). With this method, the time is greatly reduced as the post cure time required to make a sample is around one hour in total. In addition, it represents a great amount of savings in tooling, as tensile testing machine is no

longer required nor the hinges or adhesive. To prevent water from making its way inside the sample during scanning in the immersion tank, the separated edges from the delamination were sealed with Epoxy resin.

### Aerogel/Epoxy Simulated Delamination

#### **First Attempt**

Initially, direct application of aerogel particles was attempted. This was immediately ruled out as a viable method, as soon as the next ply was applied the majority of the aerogel was expelled, due to the extremely low density and hydrophobic nature, from the midplane leaving only trace amounts adhered to the surfaces. The panel was cured as per the normal procedure despite this, though as expected no signature of damage was detected.

#### **Aero-Epoxy**

In an effort to keep the aerogel contained, it was decided to attempt to contain it within another material then apply it to the panel. Since it was also desired for the inclusion material to be as similar as possible to the surrounding pre-preg matrix so the effect of the aerogel on its own could be investigated, epoxy resin was chosen to be mixed in with the aerogel. Pouring the aerogel particles into a container filled with epoxy then manually mixing them together by hand using a stirring stick proved to be relatively effective at capturing the aerogel, though not time efficient nor material efficient as the aerogel still tended to drift away from the mixing cup. Seeking to further contain the materials and expedite the mixing process, cups with lids and a stand mixer were employed. Figure 13 shows the basic process flow. Once mixed the aerogel-epoxy mixture, or Aero-Epoxy, can be applied as desired with a viscosity resembling that of the epoxy itself.

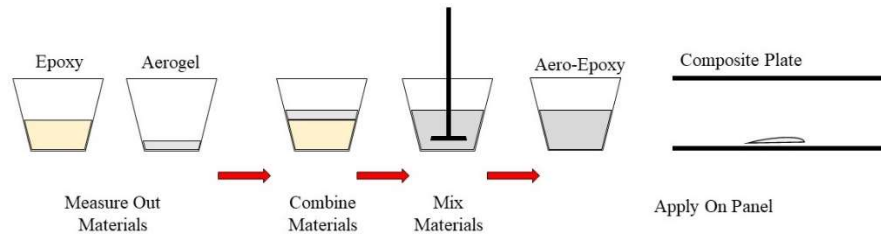


Figure 13: Aero-Epoxy Manufacturing Flow Chart

### Aero-Epoxy: Immediate Application

With an effective and efficient method of aerogel application laid out, the first step was to determine if the Aero-Epoxy would produce a noticeable damage signature under NDE inspection. A section of pure epoxy was included on the sample to compare with the Aero-Epoxy section to see if the Aerogel was having an appreciable effect or if the response was due to the epoxy alone. After achieving promising results, the effect of the extent of polymerization of epoxy was studied to arrive at the best material state for the simulation of damage.

### Aero-Epoxy: Partially Cured Epoxy

After reviewing the results of the first test, it was decided that the excessive spreading of the Aero-Epoxy needed to be controlled if it were to be a viable method of creating controlled synthetic damage. For the next experiment everything was left unchanged except for the application time. Instead of applying the mixture immediately, the epoxy was allowed to partially set (also called the green state) before applying it at the midplane. This significantly reduced the spread after pressing and curing to a point where it could be used for good approximation of amorphous damage regions.

### Aero-Epoxy: Fully Cured Epoxy

In a final attempt to even further restrain the movement of the material during the curing cycle, the epoxy was allowed to fully set prior to placing it in the laminate. However, leaving it to solidify without added pressure would mean that it would be relatively thick when set and would locally change the laminate thickness heavily when placed in between plies. The thickness of the Aero-Epoxy sheet was reduced by first placing the uncured mixture between two sheets of release ply on a flat metal plate. Then a heavy weight was placed on top to apply pressure to spread the Aero-Epoxy as thin as possible. Post-cure thickness was measured to be just above one millimeter, furthermore the Aero-Epoxy sheet could be easily cut/shaped with a utility knife. Squares were made from the sheet (as well as a pure epoxy version made shortly after the first sheet) then included in CFRP sample for inspection. No further spread was observed with this method.

### Epoxy to Aerogel Ratio

After observing promising results with the Aero-Epoxy, it was desired to explore the relationship between the ratio of epoxy to aerogel and the signature it presents in both ultrasonic damage reflection amplitude and attenuated backwall reflection amplitude. Using the standard mixing procedure defined earlier, samples were made containing ratios from 20% aerogel to 200% aerogel by volume. While forming each of the mixtures a curious behavior was found in the mixture. As the ratio of aerogel was increased, the viscosity of the Aero-Epoxy mixture increased noticeably as well. As the Epoxy to Aerogel ratio approached 1:1.5 it became difficult to mix the Aero-Epoxy, the resistance becoming too much for the mixer to handle. 1:2 represents the upper limit of mixture as at that point the mixture

becomes putty like in consistency and no longer takes on any more Aerogel. This behavior could be used to address the spreading problem mentioned previously.

#### Aero-Epoxy Signal Variation Sample

Previous scans of Aero-Epoxy samples revealed a relative uniformity in the defect response, but in real world the defects may be non-uniform in how they reflect and attenuate the Ultrasonic signal, especially delaminations. To study the damage response variation, three different ratios (1:0.2, 1:0.4, 1:0.6 Epoxy to Aerogel) of Aero-Epoxy were randomly distributed onto the midplane with the anticipation of emulating the variability found in many forms of defects. No change was made to the curing process.

#### **Material Characteristic Sample Blocks**

When constructing the ratio variation samples, more Aero-Epoxy mixture was made than was needed to be applied to each sample, and the excess was saved for the purposes of learning more about the mixture itself. The Aero-Epoxy excess was poured into ice-cube tray coated with FreKote and Fiberglast, and allowed to cure. These cubes were then removed from the tray and cut with a water-jet so that there would be two flat parallel sides to place Ultrasonic Transducers for TTU investigation later.

## CHAPTER 4. RESULTS

## Initial Trials

As assumed prior to scanning, ultrasonic scans of the first aerogel panel where the aerogel was simply sprinkled onto the surface showed no obvious signs of the inclusion or other damage markers. Though the standard probe was the 0.25 inch 5 MHz transducer, a 0.25 inch 10 MHz transducer was used to scan the panel again to verify that no damage could be seen in case a shorter wavelength was necessary to pick up the affected regions. However as can be seen in Figure 14, this was not the case. It was clear that the particles had spread out far too much to be noticed, and that a new method would need to be developed for the application of the aerogel to the laminate.

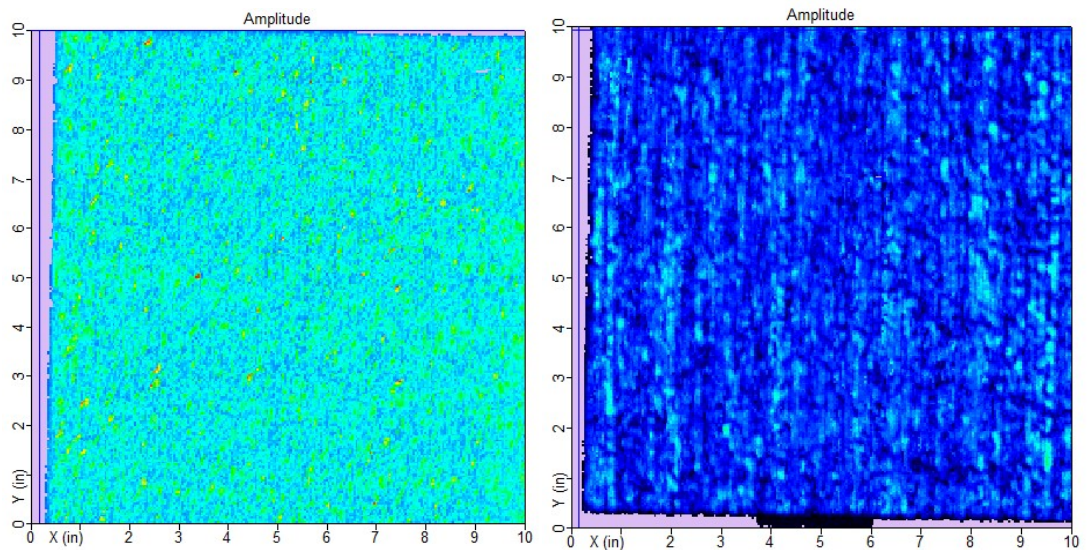


Figure 14: Immersion Scan Results of First Aerogel Trial (5 MHz Left, 10 MHz Right)

## Shape Control Trials

Once it was known the Aerogel was able to be contained within the laminate due to the addition of an epoxy resin binder, a new set of samples were made to explore the ability for the fabricator to choose the shape of the final defect during the panel layup process.



### Immediate Application

The first Aero-Epoxy press (with a pure epoxy region for comparison) was scanned and found to have the response shown in Figure 15. In this image one can see that the upper region of the image where the Aero-Epoxy was placed gives off a slightly higher amplitude response than that of the pure epoxy region below it. It can also be seen that in comparison to the pre-pressed image both regions have significantly spread compared to their original rectangular shapes.

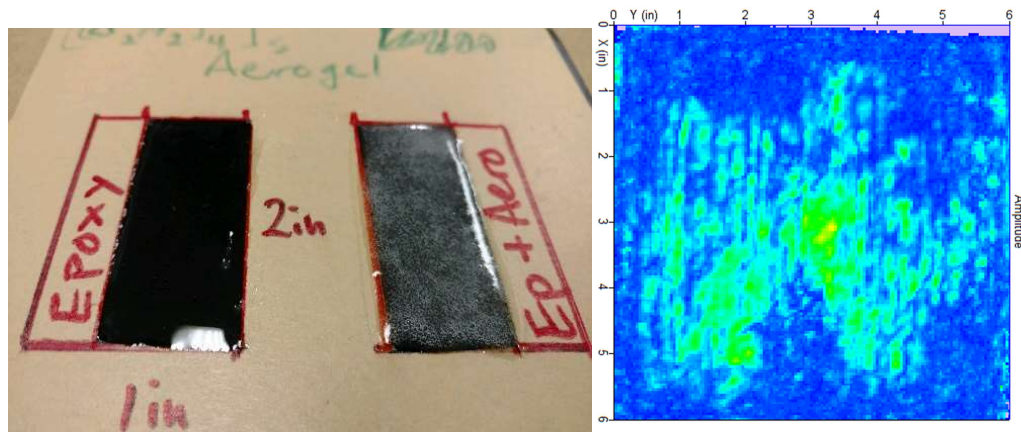


Figure 15: a.) Aero-Epoxy Sample Prior to Assembly b.) Immersion Scan Results

### Aero-Epoxy Panel

### Partially Set Epoxy

To reduce the spread of the epoxy during pressing, it was brought to green state (but yet still be pliable) before applying it to the laminate as in Figure 15. Additionally, more Aerogel was added to the Aero-Epoxy mixture to see if the difference in amplitudes could be made to be more pronounced. Once scanned, it was seen that the spread was indeed reduced and that the difference between the upper Aero-Epoxy region and the lower pure Epoxy region was quite dramatic. Still, the initial rectangular regions of additive had cured into

much more amorphous blobs during pressing and so one final test was carried out to see if it was possible to exactly control the shape of the defect.

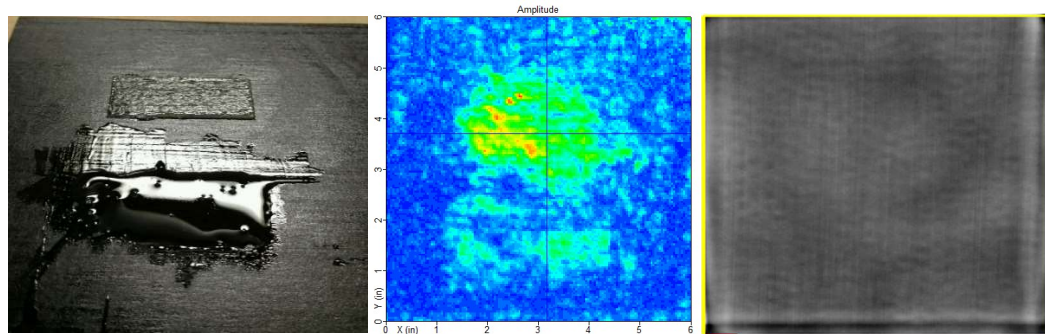


Figure 16: a.) Partially Cured Mixture and Epoxy Prior to Assembly b.) Immersion Scan of Panel c.) Thermographic Scan of Panel

### Fully Set Epoxy Sheets

Since allowing the epoxy to begin to set reduced the distortion of the originally epoxy shape, the next logical step was to fully cure the epoxy prior to placing it in the laminate layup. To control thickness, it was placed under pressure during the setting period. The resulting thin sheets of Aero-Epoxy and pure Epoxy were then cut into squares, rectangles, and a few random designs then added to the CFRP (Figure 17). Once again, the Aero-Epoxy portions displayed more distinct signatures than the pure epoxy. As hoped, the size and shape of the defects could then be precisely controlled whilst maintaining the effects of the aerogel addition. In future use, it would be pertinent to continue to reduce the thickness mismatch of the sheets and the plies as the sheets were just slightly thicker than one millimeter while each ply was on the order of 0.125 mm thick before the laminate was put in the press for final cure.

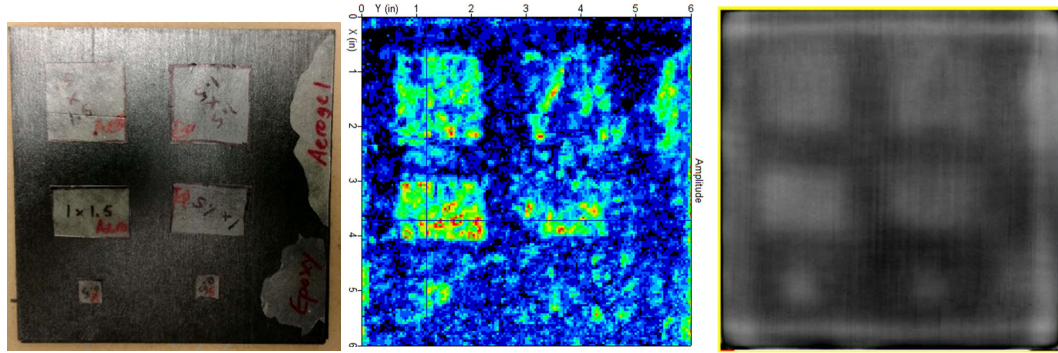


Figure 17: a.) Solid Aero-Epoxy and Pure Epoxy Sheets On Midplane Prior to Assembly b.) Immersion Scan of Solid Epoxy Sample c.) Thermographic Scan of Solid Epoxy Sample

### Exploration of Content Ratio Effects

When reviewing the results of the partial set test, it seemed as though increasing the amount of aerogel contained in the epoxy increased the amplitude of the signal attained when scanned. A new set of tests was designed to explore the relationship between the ratio of Epoxy to Aerogel and the damage signal and backwall attenuation. Using a constant amount of Epoxy and increasing amounts of Aerogel, several ratios from 1:0.2 Epoxy:Aerogel to 1:2 Epoxy:Aerogel were mixed and samples created. During the process of creating the mixtures it was noted that there was an increase of mixture viscosity with each increase in ratio, to a point where the mixture became so thick in consistency that it could no longer be mixed via the electric mixer and no more aerogel could be added.



Figure 18: Progression of Aero-Epoxy Viscosity a.) Less Than 1:1 b.) Between 1:1 and 1:2 c.) 1:2 and Greater

A-Scans from the locations in the CFRP containing Aero-Epoxy were gathered for each sample. Peak amplitudes for the damage region and backwall were gathered and plotted versus increasing ratio of inclusion as seen in Figures 19-20. The amalgamation of graphs in figure 19 does not show a clear picture of the behavior occurring with each increase. In figure 20 no clear trend can be seen in the data, as the damage signal peak amplitude varies across the ratios quite a bit. In contrast, the backwall amplitude does not vary near as much along the spread of ratios. In general, most damages present both a prominent signal somewhere between the front and back plies and a corresponding reduction of the backwall signal due to the reflection and scattering the incoming energy. Taking this into account, the ratio of 1:1 displayed the best combination of defect amplitude and backwall reduction and was chosen as the metric to compare with existing damages to determine how well they could be approximated with Aero-Epoxy.

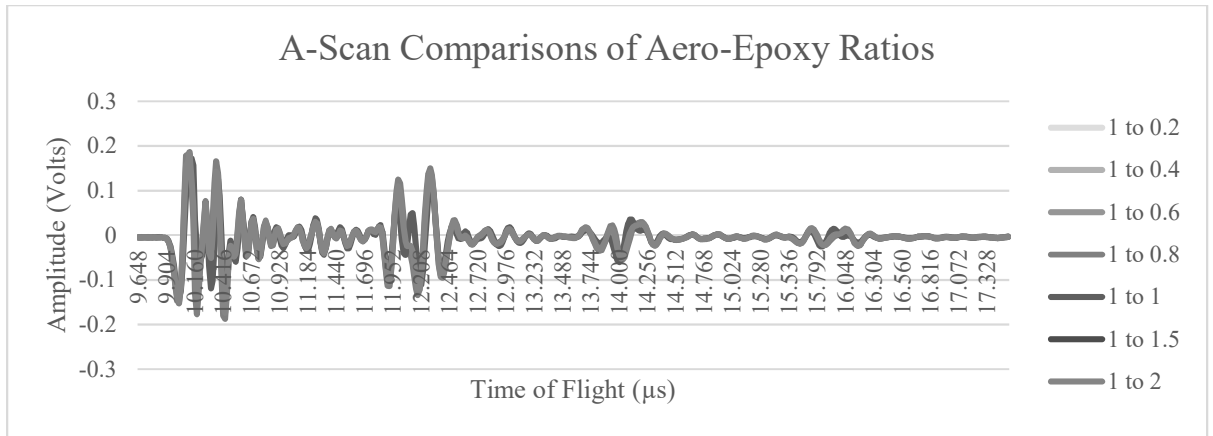


Figure 19: A-Scan Comparison of Aero-Epoxy Ratios

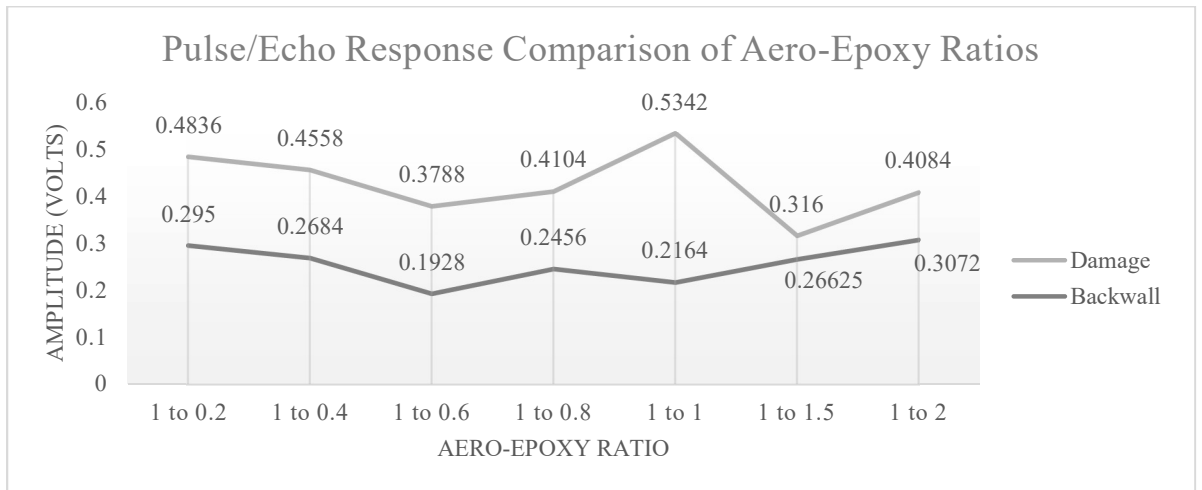


Figure 20: Graph of Amplitudes of Damage Signals and Backwall Signals for Aero-Epoxy Ratios

### Signature Variability Test

Each of the Aero-Epoxy samples, though different in signature in terms of amplitudes, did share the fact that they were very uniform in signal across the defect (see Figure 21). True damage often does not have such uniform appearances, so using the results from the ratio experiments a method of emulating such variability was created. The first three ratios (1:0.2, 1:0.4, and 1:0.6) were distributed randomly in the CFRP sample, and with each

having a different signature it was expected to show the desired trait. Figure 21 shows the behavior of standard Aero-Epoxy panels, while Figure 22 shows the results of this test.

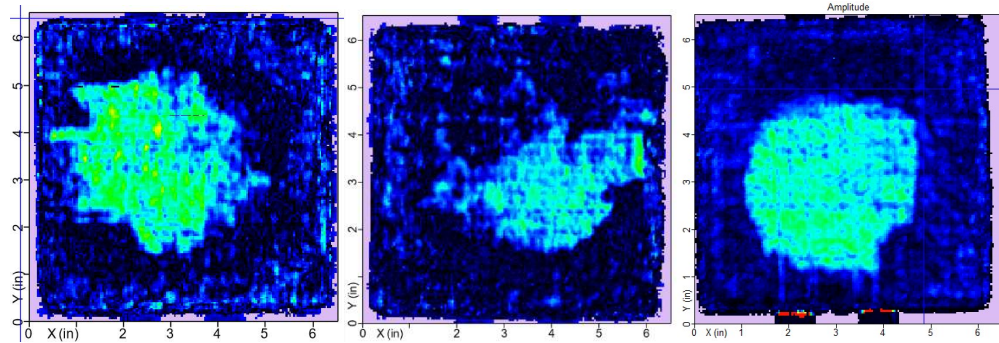


Figure 21: Example of Uniform Signature in Aero-Epoxy Samples a.) 1:1 b.) 1:1.5  
c.) 1:2

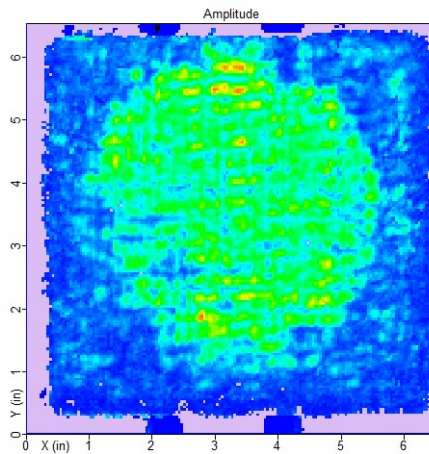


Figure 22: Immersion Scan Showing Variability of Signal Using Multiple Aero-Epoxy Ratios

The variation desired was partially achieved although much of the sample was uniform as with previous samples and spreading had occurred lessening the effect of the distribution. This method, when used in conjunction with the method of partial

polymerization prior to application could provide more pronounced effect by limiting the spread and slightly increasing the thickness and concentration of the Aero-Epoxy layer.

### Physical Characteristics

Though the responses within CFRP in response to ultrasonic and thermographic inspection were known, not much about the characteristics of the material mixture itself was known. Of particular interest are the acoustic impedance and coefficient of reflection, two parameters that determine much of how the material will appear under Ultrasonic Inspection. Using the water immersion density measurement technique, the density of each of the prepared sample blocks (including a pure epoxy block) was measured and recorded. Through-transmission was used to determine the wave speed of each sample by recording the time at which the first signal ping occurs (Time of Flight) and the thickness of the block itself. The through transmission method was used since the aerogel/epoxy material is in general very attenuative. Then, using the wave speed and density, the impedance was calculated using the simple formula:

$$Z = \rho v$$

With the impedances now known, the coefficient of reflection could be calculated, as it is based on the impedance mismatch between the mediums the signal is passing through.  $Z_2$  refers to the impedance of the second medium (in this case Aero-Epoxy block) and  $Z_1$  refers to the impedance of the traveling medium (air, water, aluminum, etc.).

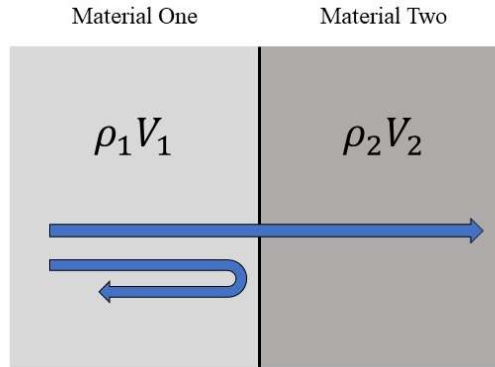


Figure 23: Diagram of Acoustic Reflection at Material Interfaces

$$C_r = \frac{\rho_2 v_2 / \rho_1 v_1 - 1}{\rho_2 v_2 / \rho_1 v_1 + 1} = \frac{Z_2 / Z_1 - 1}{Z_2 / Z_1 + 1} \quad (\text{Achenbach})$$

Table 1 contains the results for each of the samples for quick reference and comparison. Addition of the Aerogel to the Epoxy seemed to have resulted in several changes from the base Epoxy characteristics. For one, there is a reduction of the wave speed through the material, up to almost 430 m/s at the 1:0.8 ratio. There is also a slight reduction in density as the ratio increases. As hoped the impedance values are smaller than with Epoxy alone but are still nowhere near that of air ( $Z_{\text{air}} = 0.000429 \times 10^6 \text{ kg/m}^2\text{s}$ ) or of Aerogel by itself ( $Z_{\text{Aerogel}} = 0.000077 \times 10^6 \text{ kg/m}^2\text{s}$ ). It should be pointed out here that this acoustic impedance of air is not the true representation of the reflection coefficient from a delamination. In a true delamination, there exists some fiber bridging which provides a path to the ultrasonic waves to pass through the interface. Moreover, the two delaminated surfaces are not clearly apart. There is some intermittent contact between these surfaces which is called “kissing bonds” and this allows a partial wave propagation across the delamination.



Table 1: Properties of Aero-Epoxy

Mix Ratio	Epoxy	1 to 0.2	1 to 0.4	1 to 0.6	1 to 0.8	1 to 1	1 to 1.5	1 to 2
Wave Speed (m/s)	2532 ±0.09%	2378 ±0.11%	2157 ±0.11%	2056 ±0.11%	2064 ±0.11%	2050 ±0.08%	2162 ±0.08%	2234 ±0.08%
Density (g/cm <sup>3</sup> )	1.135	0.996	0.919	0.879	0.870	0.878	0.946	0.980
Impedance (kg/m <sup>2</sup> s x 10 <sup>6</sup> )	2.874	2.368	1.982	1.807	1.795	1.800	2.046	2.189
C <sub>r</sub> (Water)	0.320	0.231	0.145	0.100	0.096	0.098	0.160	0.193
C <sub>r</sub> (Aluminum)	-0.711	-0.755	-0.791	-0.808	-0.809	-0.808	-0.785	-0.772
C <sub>r</sub> (CFRP)	-0.183	-0.274	-0.354	-0.394	-0.397	-0.396	-0.341	-0.310

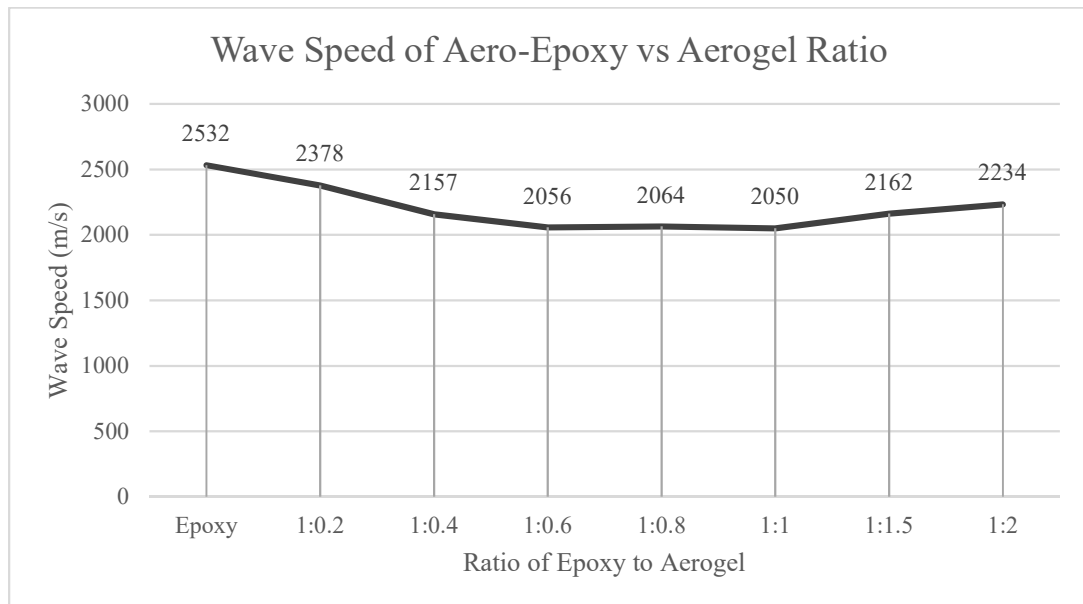


Figure 24: Wave Speed of Aero-Epoxy as Aerogel Ratio Increases

To learn more about the Aero-Epoxy mixture itself microscopy was performed on a few samples of the Aero-Epoxy. The goal was to better understand the wave speed behavior that was observed from the TTU measurements. As seen in Figure 25, the Aerogel powder is an amalgamation of jagged crystalline particles. At 1:0.2 the Aerogel particles can be seen coating the outer edges of small air bubbles spread out within the epoxy. As the ratio increases (1:0.8 shown), the density of these small orbs increases with larger bubbles beginning to form. By 1:2, the bubbles had grown in size but spacing between them had also increased. It seems as though at low amounts of Aerogel, the inclusions begin to reduce the wave speed. As more aerogel is included, more of the bubbles begin to form, further reducing the wave speed. Finally, as the ratio approaches 1:2, the bubbles increase in size but the relative density of aerogel inclusions within the epoxy decreases leading to the increase in wave speed seen from the TTU measurements



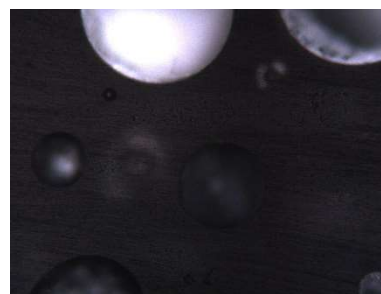
Aerogel Particles



1:0.2 Aero-Epoxy



1:0.8 Aero-Epoxy



1:2 Aero-Epoxy

Figure 25: Microscopy of Aerogel Particles and Aero-Epoxy Samples

## Similarity to Other Defect Types

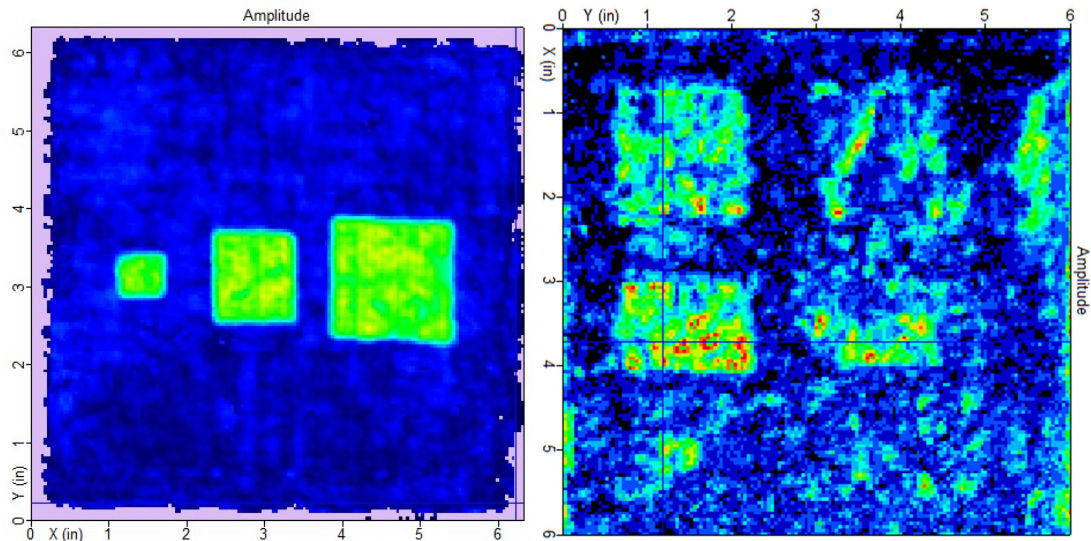
**Film Inserts**

Figure 26: Visual Comparison of Film Insert Defect and Solid Sheet Aero-Epoxy Sample

Film or backing paper inclusions are characterized by well-defined edges and a relatively consistent signature across the defect. They stand out quite clearly from the surrounding laminate signal. The Aero-Epoxy mixture that seems to replicate this form of damage the best when the mixture is applied once it is fully cured. The material can be cut into any desired shape and size and is also fairly consistent in signature across each of the inserts, though it may not appear that way. The color grading can be changed and customized with the analysis software used, so the visual appearance is generally only useful for the purposes of comparing sizing and geometry and A-Scan data should be used for more in-depth investigation of the signals. Figure 25 shows that the same damage can appear to have a higher amplitude signal response simply by altering the coloring on the image.

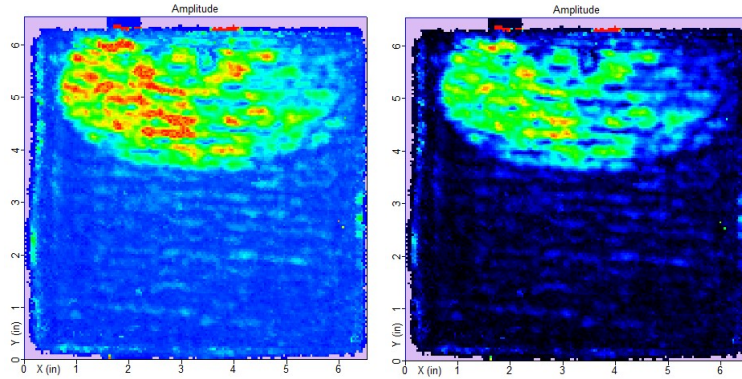


Figure 27: Difference in Apparent Amplitude Based on Color Grading

It is worth noting that the manufacturing time for film inserts is faster than the time for the full process of creating the solidified Aero-Epoxy sheet due to the curing time required for the mixture. However, if some of the mixture was reserved from other applications, it could be hardened and then used for this process. In terms of attenuation and signal, the waveform response of 1:0.8 Epoxy to Aerogel is very close to that of the film inserts.

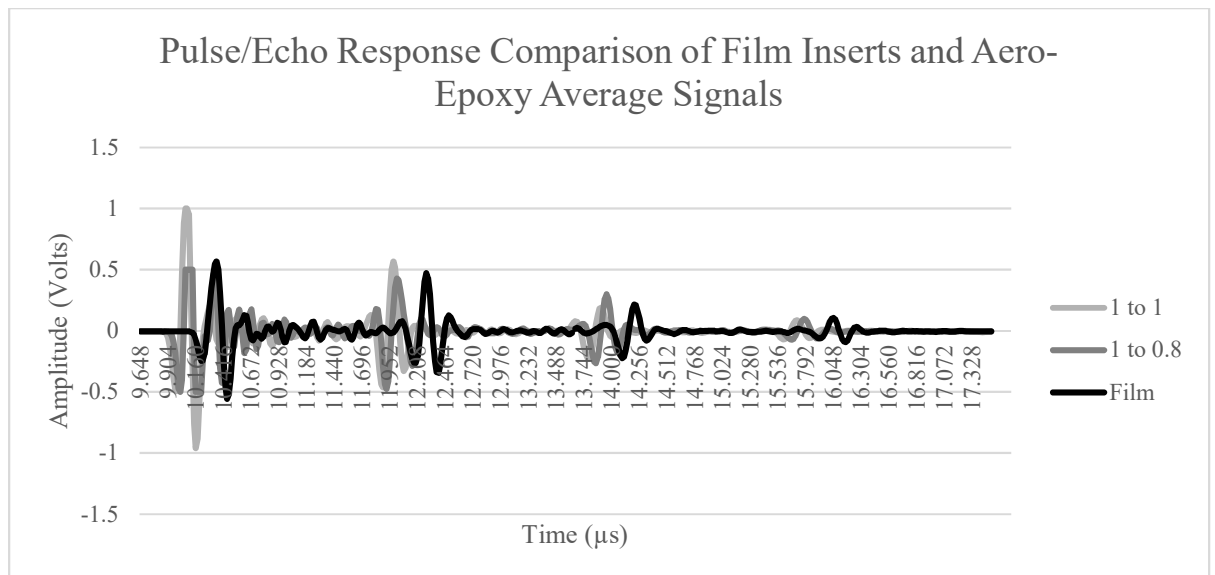


Figure 28: Signature Comparison of Film Insert, 1:0.8 Aero-Epoxy, and 1:1 Aero-Epoxy Samples

## Baking Soda Inclusions

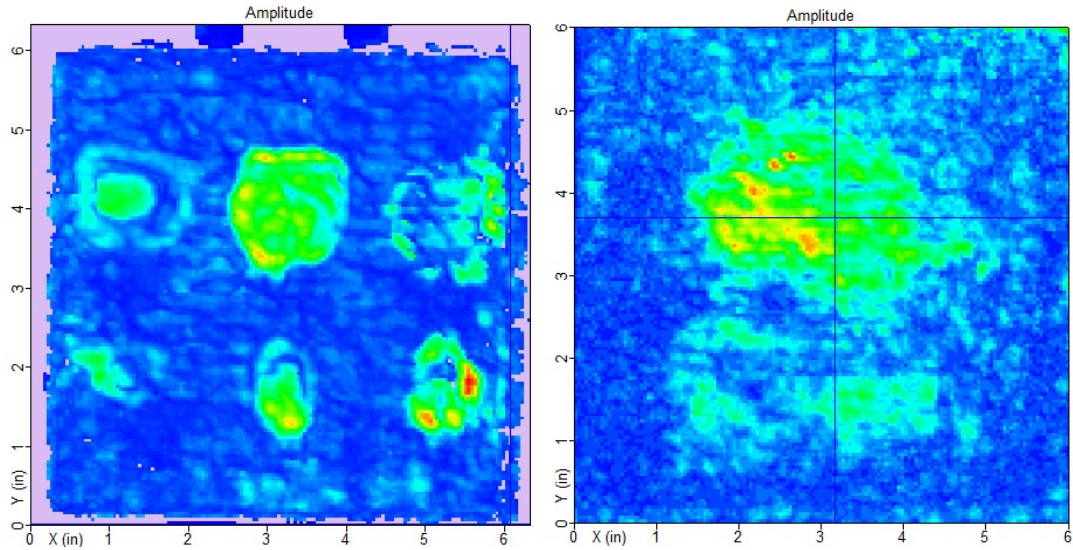


Figure 29: Visual Comparison of Baking Soda and Partially Cured Aero-Epoxy Samples

Unlike Film, baking soda appears as amorphous blobs even when care is taken to neatly place it in square piles during the manufacturing process; it simply spreads during curing/pressing. Due to the varying thickness of the inclusion, there is more variability in the signal peaks leading to a more non-uniform look. This could be achieved with the partial curing method augmented with the variability method, partial cure to hold the shape and variability to achieve the non-uniform look of the real defect. The 1:1 ratio and 1:0.8 ratio of Aero-Epoxy captures the signature of Baking Soda defects fairly well, but 1:1 would be preferred due to increased viscosity of mixtures with higher percentages of Aerogel which leads to less spread during curing.

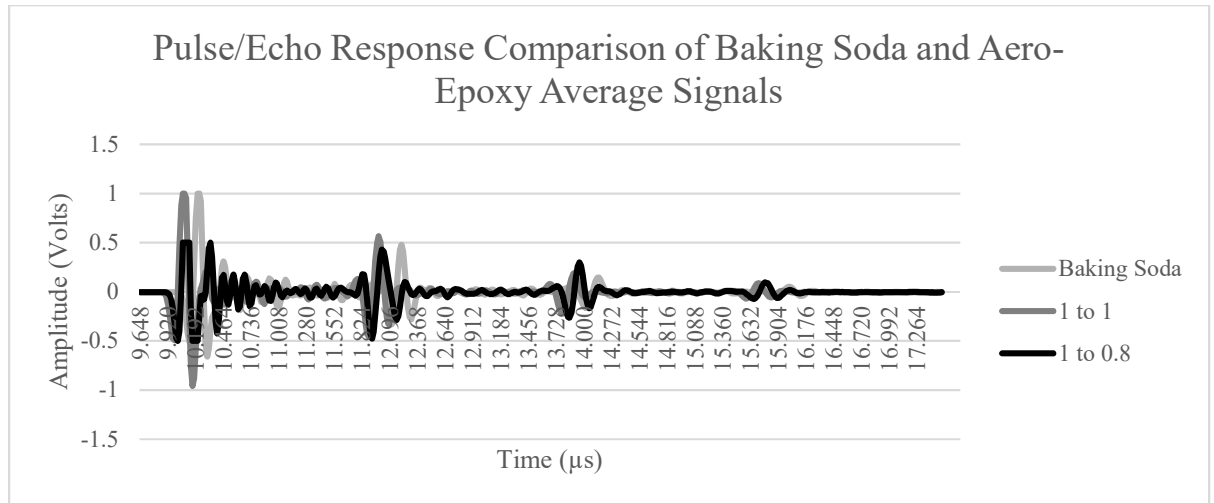


Figure 30: Signature Comparison of Baking Soda, 1:0.8 Aero-Epoxy, and 1:1 Aero-Epoxy Samples

### Impact Damage

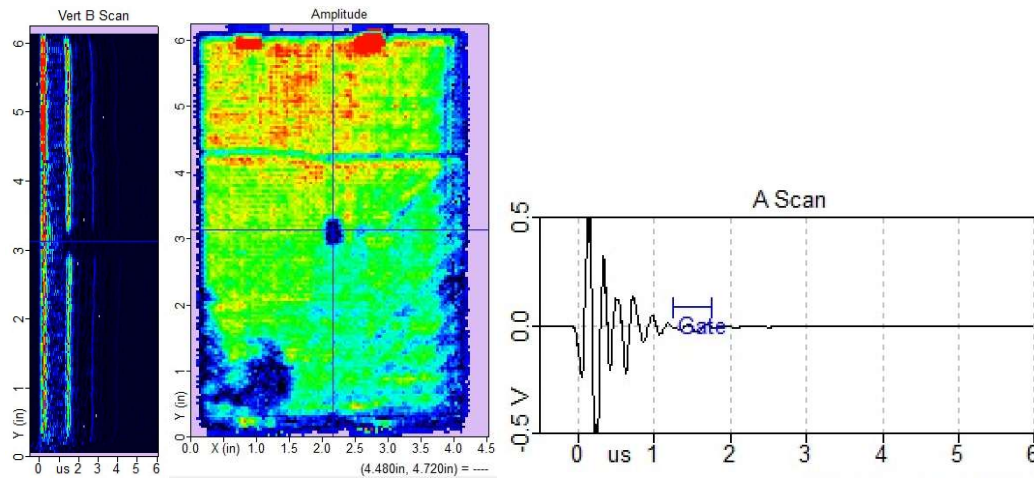


Figure 31: UT Inspection Results of a Blunt Impact on CFRP (B-Scan, C-Scan, A-Scan Left to Right)

Impact damage in CFRP, as mentioned previously, is primarily matrix crushing with some delamination occurring in a radial pattern amount the impact site. From the Pulse/Echo Immersion Scan, shown in Figure 29, it is immediately clear that the signature of this type of damage is unlike any of the other types discussed. In the B-Scan image there is no indication

of damage between the front wall and backwall of the sample, but instead a lack of signal from the backwall itself over the location of impact. A-Scan inspection of this region confirms that the signal is either highly attenuated or simply not received due to the damage. Aero-Epoxy is generally able to mimic inserts and delamination due to it appearing as a signal between the front wall and backwall with similar attenuation to the defect types it is simulating. With current methods presented here, emulating impact damage with Aero-Epoxy is not possible. Perhaps if a layer or even two of Aero-Epoxy were placed very near to the front surface of laminate as well as the bottom, leaving a small gap where the “impact” is the relative intensity of the signals plus the attenuation of the Aero-Epoxy could make the uncovered region appear as though it were “missing” as in the true impact case. Still, due to the simplicity of the current method of manufacturing impact damage, such a method using Aero-Epoxy would be impractical to say the least.

### True Delaminations

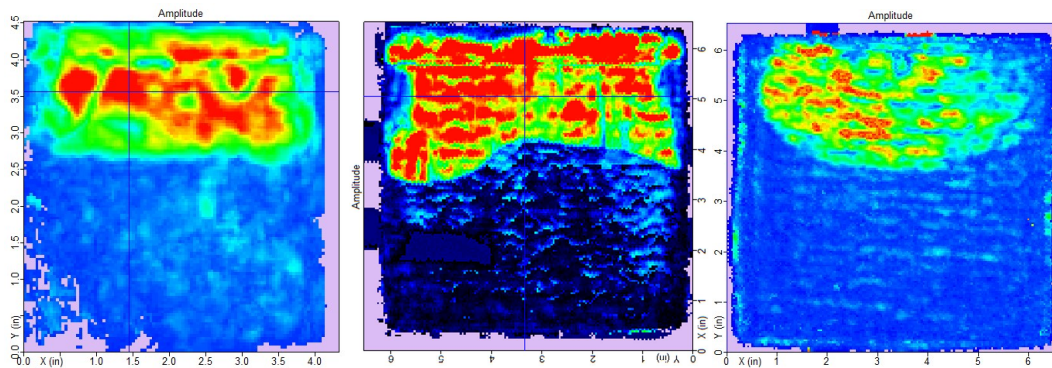


Figure 32: Visual Comparison of Teflon Delamination, Aluminum Delamination, and Aero-Epoxy Simulated Delamination (Left to Right)

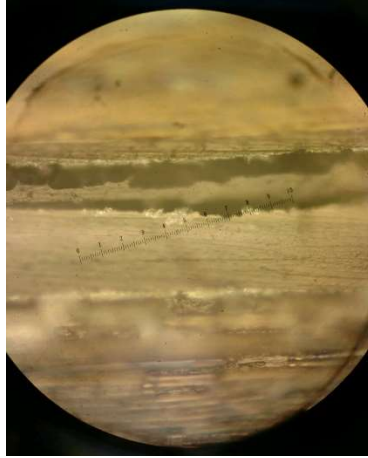


Figure 33: Micrograph of Delamination

Of all the defect types examined in this paper, delaminations possess the greatest variability in their signature across the damaged region as evidenced by Figure 30. The peak amplitude of the damage signal found from UT inspection is of larger magnitude coupled with a large amount of attenuation due to large amounts of reflection and scattering leading to a largely diminished backwall signal. In Figure 32, a comparison of the average signal response of the true delamination and the Aero-Epoxy simulated version is made. The simulated version contained 1:0.6 Aero-Epoxy and though it matches visually, it does not come very close in matching the waveform. Using higher ratios of Aerogel, a much closer match was found. At 1:1, the Aero-Epoxy mixture's average signal came much closer to a match of the true delaminations signal response (see Figure 32). Using this ratio of Aero-Epoxy it appears that an effective and efficient synthetic delamination can indeed be produced.



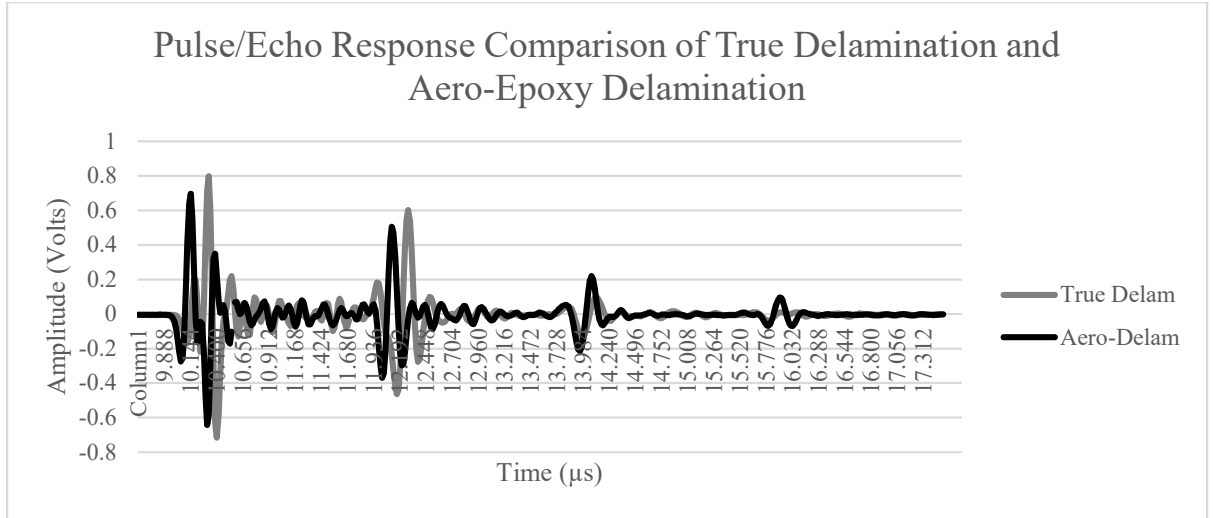


Figure 34: Signature Comparison of True Delamination and Aero-Epoxy Simulated Delamination

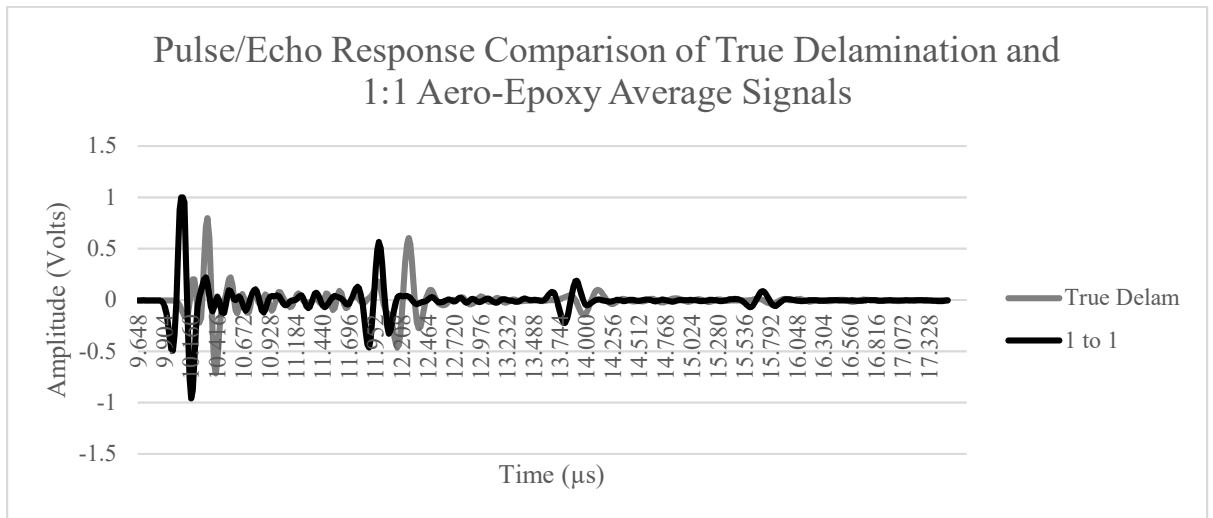


Figure 35: Signature Comparison of True Delamination and 1:1 Aero-Epoxy

## CHAPTER 5. CONCLUSION

It has been demonstrated that Aerogel when mixed with Epoxy resin is indeed capable of emulating delaminations as well as foreign body inclusions within CFRP composites, though falls short on recreating barely visible damage from impacts. By changing the ratio of Epoxy to Aerogel, the signals can be tailored towards specific types of damage, almost matching film inserts and baking soda inclusions exactly in acoustic response under ultrasonic investigation. The 1:1 ratio of Aero-Epoxy can closely emulate the amplitudes of the damage and backwall in addition to the visual appearance of a true delamination. Due to the simple nature of manufacturing Aero-Epoxy and applying it to a test sample, the method greatly saves in time and cost. Instead of several hours per sample to create a Teflon or Aluminum based delamination, an Aero-Epoxy synthetic analog can be created in much less time and is ready to use immediately after the curing cycle is complete. Expensive manufacturing equipment such as a tensile testing fixture would not be required to make the standards. Additionally, because the Aero-Epoxy can be spread anywhere in the panel, the geometry restrictions that bound the capabilities of the previous delamination methods are no longer an issue allowing for synthetic delaminations to be manufactured in the middle of a composite laminate and also in between any layer. The material itself is highly tailorable from density and acoustic impedance to the shape of the inclusions (completely amorphous or highly defined shapes). It is also cheap to manufacture, requiring only some basic mixing equipment, epoxy resin, and aerogel. As for foreign body inclusions and impact damage, the current fabrication methods are still more efficient in time required and cost than the Aero-Epoxy methods shown here.

Moving forward with the research it would be pertinent to investigate whether it is possible to further reduce the impedance of the material to make it much closer to that of air. The closer the impedance is to air, the more the signal will match that of a delamination. This could perhaps be achieved by finding a much less dense binding material to replace the epoxy resin, so the resulting overall density would be reduced. It might also be interesting to see if there could be additional additives that could improve the performance of the mixture and prevent adhesion to the surrounding laminate, since the adhesion allows for signal transmission through the two mediums that is usually hindered by real damage.

## REFERENCES

- A. Soleimani Dorcheh, M.H. Abbasi. "Silica Aerogel; Synthesis, Properties, and Characterization." *Journal of Materials Processing Technology* (2008).
- Achenbach, J. D. *Wave Propagation In Elastic Solids*. North-Holland Publishing Company, 1973.
- "Appendix A: Typical Acoustic Properties of Tissues." Azhari, Haim. *Basics of Biomedical Ultrasound for Engineers*. Wiley-IEEE Press, 2010.
- B. Sainz, J.M. Bernado, V. Cortes, C. Valdecantos. "Ultrasonic Inspection of Advanced CFRP Structures By Computer Controlled Pulse-Echo Technique." *Impact of Emerging NDE-NDI Methods on Aircraft Design*. Brussels, Belgium: Advisory Group for Aerospace Research and Development, 1990. 8.
- B.D. Agarwal, John L. J. Broutman. *Analysis and Performance of Fiber Composites*. NY: Wiley & Sons, 1980.
- Center, NDT Resource. *Accoustic Properties for Metals in Solid Form*, [https://www.nde-ed.org/GeneralResources/MaterialProperties/UT/ut\\_matlprop\\_metals.htm](https://www.nde-ed.org/GeneralResources/MaterialProperties/UT/ut_matlprop_metals.htm). n.d. August 2017.
- Dennis P. Roach, Thomas M. Rice, Kirk A. Rackow. *A Quantitative Assessment of Conventional Nondestructive Inspection Techniques for Detecting Flaws in Composite Laminate Aircraft Structures*. Albuquerque, NM: Sandia National Laboratories, 2016.
- Garrett, Ramon A. *Effect of Manufacturing Defects and Service-Induced Damage on the Strength of Aircraft Composite Structures*. Philadelphia: American Society for Testing and Materials, 1986.
- Hahn, Stephen W. Tsai. H. Thomas. *Introduction to Composite Materials*. Lancaster, PA: Technomic Publishing Co., 1980.
- Hrubesh, Lawrence W. "Aerogel Applications." *Journal of Non-Crystalline Solids* (1998).

- Iddings, F. A. *NDI Oriented Corrosion Control for Army Aircraft: Phase I -- Inspection Methods*. San Antonio, TX: Southwest Research Institute, 1989.
- International, ASTM. "D2563-08: Standard Practice for Classifying Visual Defects in Glass-Reinforced Plastic Laminate Parts." 2015.
- . "D2734-16: Standard Test Methods for Void Content of Reinforced Plastics." 2017.
- . "D6115-97 Standard Test Method for Mode 1 Fatigue Delamination Growth Onset of Unidirectional Fiber-Reinforced Polymer Matrix Composites." 2017.
- . "E2533-17 Standard Guide for Nondestructive Testing of Polymer Matrix Composites Used in Aerospace Applications." 2017.
- Joseph S. Heyman, William P. Winfree. "Advanced NDE Techniques for Quantitative Characterization of Aircraft." *Impact of Emerging NDE-NDI Methods on Aircraft Design Manufacture and Maintenance*. Brussels, Belgium: Advisory Group for Aerospace Research and Development, 1990. 22.
- K.L. Reifsnider, E.G. Henneke, W.W. Stinchcomb, J.C. Duke. *Damage Mechanics and NDE of Composite Laminates*. NY: Pregamonn Press, 1983.
- R. Gerlach, O. Kraus, J. Fricke, P.-Ch. Eccardt, N. Kroemer, V. Magori. "Modified SiO<sub>2</sub> Aerogels as Acoustic Impedance Matching Layers in Ultrasonic Devices." *Journal of Non-Crystalline Solids* (1992).
- Tsai, Stephen W. "Mechanics of Composite Materials Part II - Theoretical Aspects." 1966.

## APPENDIX: ADDITIONAL SAMPLE IMAGES

## Film Inserts

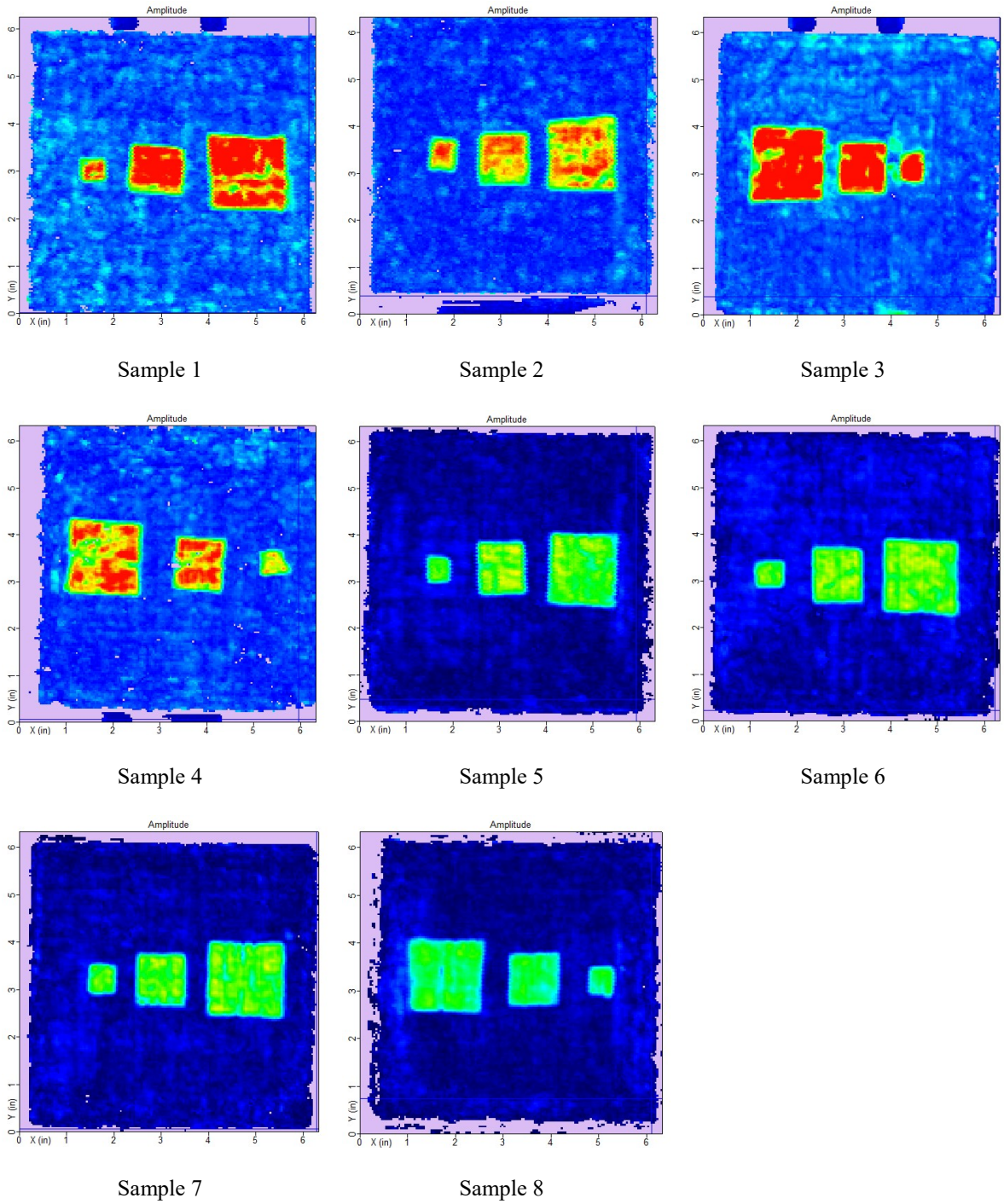
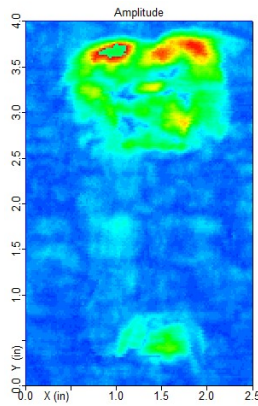
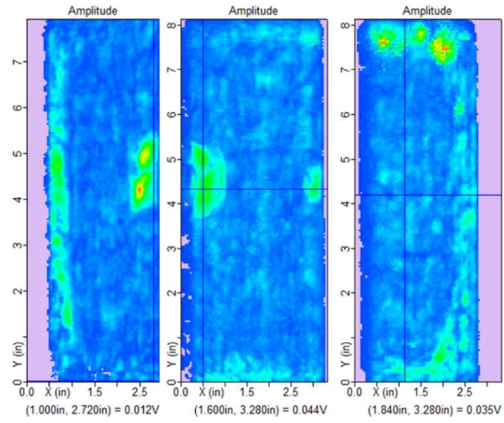


Figure 36: Pulse/Echo UT C-Scans of Additional Film Insert Samples

**Baking Soda Inserts**



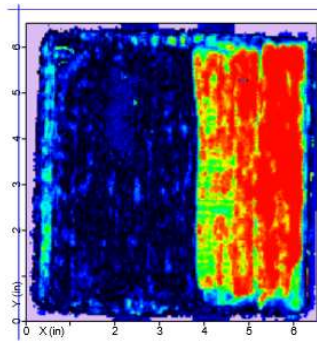
Sample 1



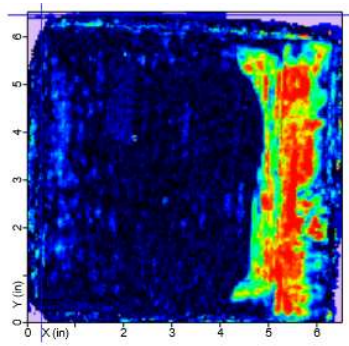
Sample 2 (16 Ply, Segmented into Three Pieces)

Figure 37: Pulse/Echo UT C-Scans of Additional Baking Soda Samples

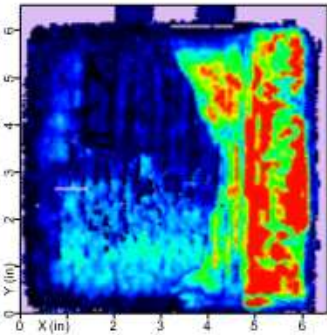
**Delaminations**



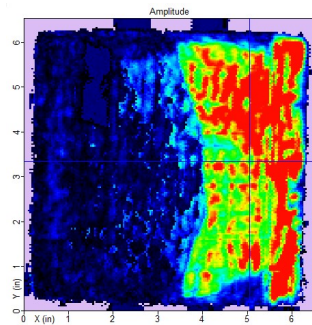
Sample 1



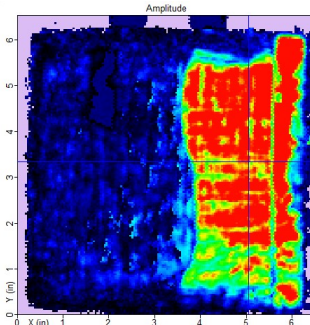
Sample 2



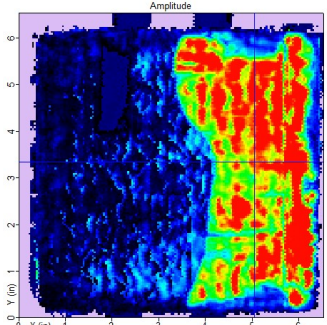
Sample 3



Sample 4



Sample 5



Sample 6

Figure 38: Pulse/Echo UT C-Scans of Additional Aluminum Delamination Samples

**Impact Damage**

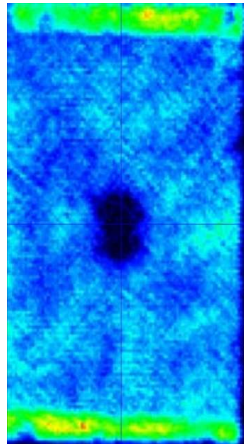


Figure 39: Pulse/Echo UT C-Scan of Additional 3J Impact Sample

**Aero-Epoxy**

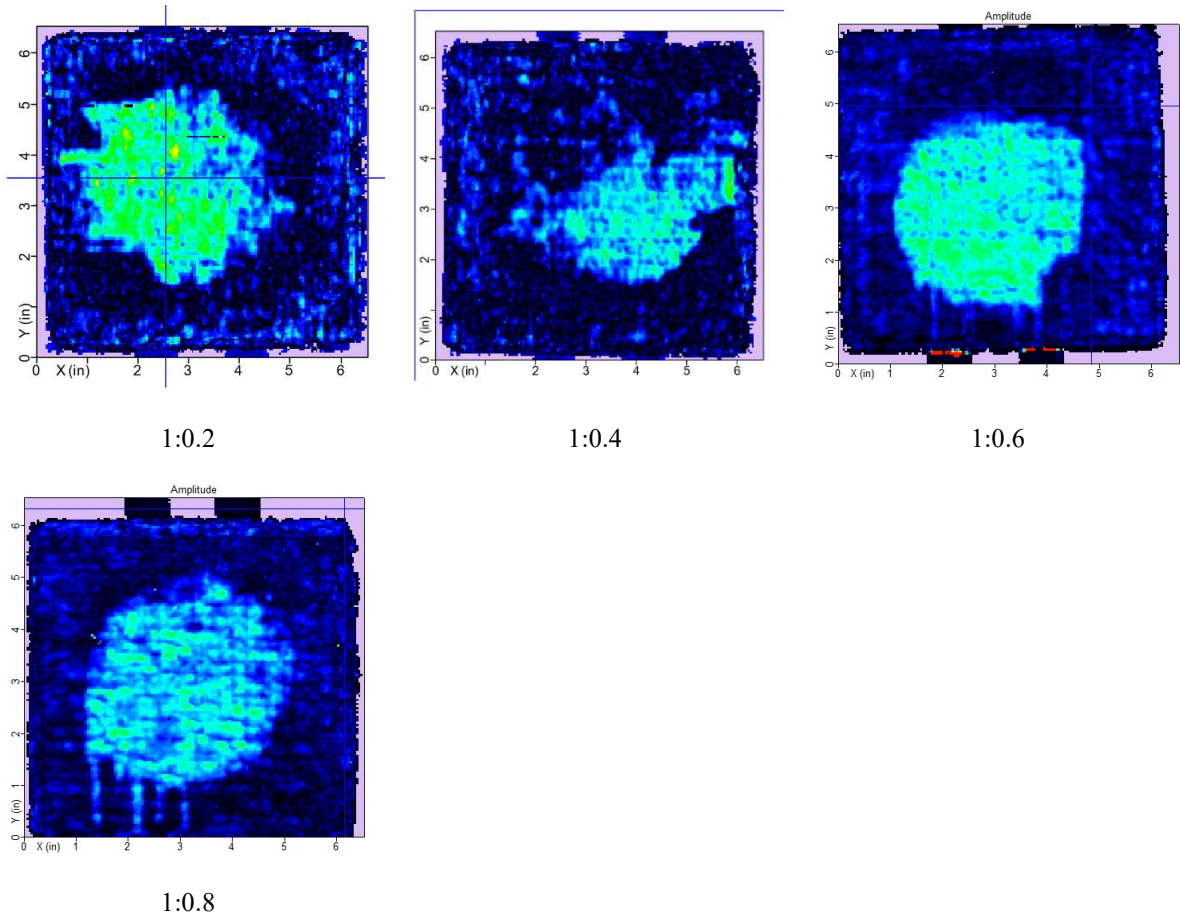
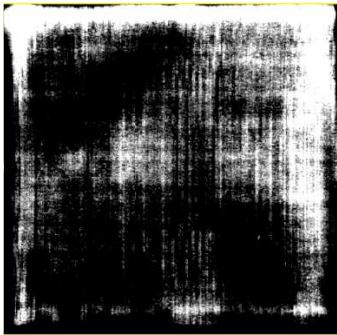


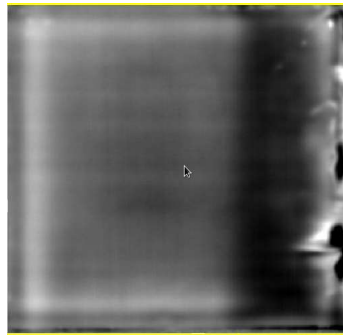
Figure 40: Pulse/Echo UT C-Scans of Various Ratios of Aero-Epoxy Samples



### Thermography



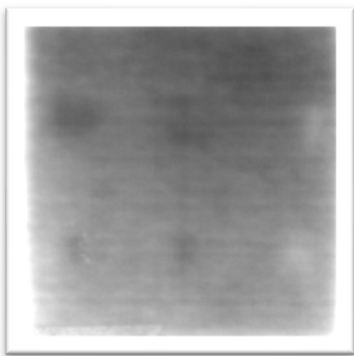
Film Insert



16 Ply Teflon Delamination



Aluminum Delamination



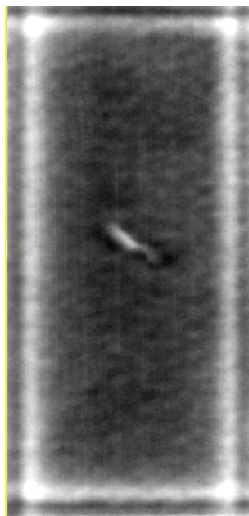
Multi-Height Baking Soda Insert



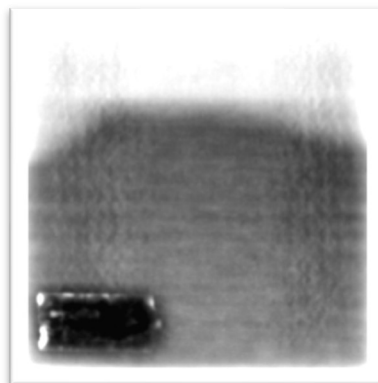
16 Ply Film Insert



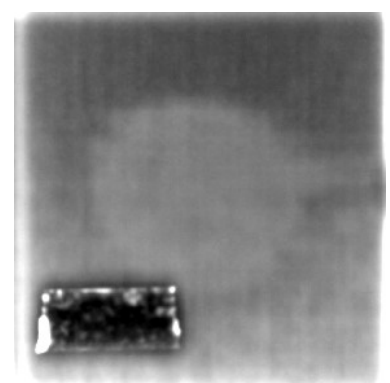
16 Ply Baking Soda (Segmented)



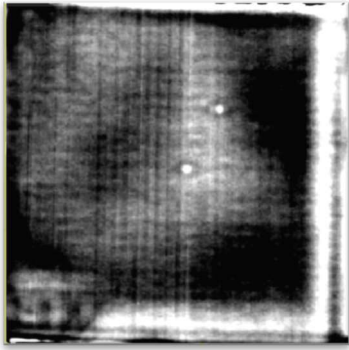
3J Impact



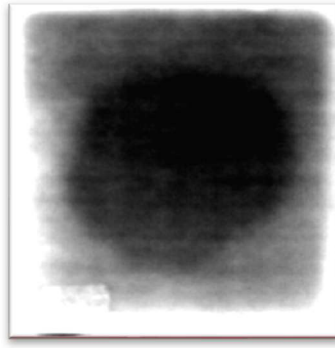
16 Ply Aluminum Delamination



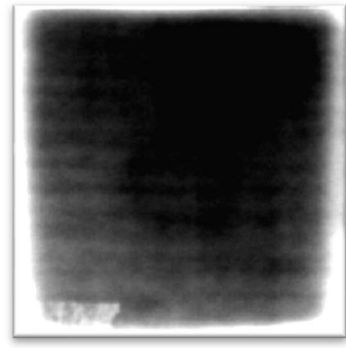
16 Ply Aero-Epoxy



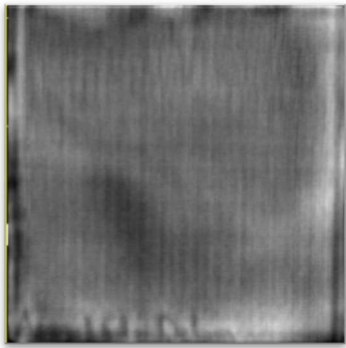
1:1 Aero-Epoxy



1:1.5 Aero-Epoxy



1:2 Aero-Epoxy



Aero-Epoxy Delamination

Figure 41: Various Thermography Scans of Samples

### Error Analysis in Wave Speed

$$v = \frac{L}{t}$$

$$\text{Step 1: } dv = \frac{dL}{t} - \frac{Ldt}{t^2}$$

$$\text{Step 2: } \frac{dv}{v} = \frac{dL}{L} - \frac{dt}{t}$$

$$\text{Result: } \frac{\Delta v}{v} = \frac{\Delta L}{L} + \frac{\Delta t}{t}$$

$$\Delta L = 0.001 \text{ inch}$$

$$\Delta t = 1 \text{e-}9 \text{ s}$$

## EXAMPLE

For the velocity of 80951.18 in/s (2056 m/s)

$$\frac{\Delta v}{v} = \frac{.001 \text{ in}}{.96 \text{ in}} + \frac{1e-9 \text{ s}}{.000021565 \text{ s}} = 0.001088 = 0.109\% = 0.11\%$$

Velocity is Reported as 2056 m/s  $\pm$  0.11%

## ACKNOWLEDGMENTS

I would like to thank my committee chair, Vinay Dayal, and my committee members, Ambar Mitra, and Stephen Holland, for their guidance and support throughout the course of this research. I would like to thank Adam Harper, Nishtha Bhatnagar, and Souleymane Hanne for their support in my research efforts. I would like to also thank my parents, Marc and Sofia Benedict, for their love and support through everything. In addition, I would also like to thank my friends, colleagues, the department faculty and staff for making my time at Iowa State University a wonderful experience.